UNITED NATIONS UNIVERSITY
UNU-GTP
Geothermal Training Programme

Orkustofnun, Grensasvegur 9,
IS-108 Reykjavik, Iceland

Reports 2014
Number 29

TEMPERATURE MODEL AND TRACER TEST ANALYSIS FOR THE RIBEIRA GRANDE GEOTHERMAL SYSTEM, SÃO MIGUEL ISLAND, AZORES

Maria da Graça Vaz de Medeiros Rangel
EDA RENOVÁVEIS, S.A.
Rua Francisco Pereira Ataíde, 1
9504-535 Ponta Delgada
PORTUGAL (AÇORES)
mrangel@eda.pt

ABSTRACT

On São Miguel Island (Azores - Portugal) EDA Renováveis, S.A., exploits the resources of the Ribeira Grande geothermal field, a 240ºC liquid-dominated reservoir, and operates two binary ORC (organic Rankine cycle) geothermal power plants, Ribeira Grande and Pico Vermelho, with a combined capacity of 23 MW_e. At present, the production from the geothermal resource represents 43% of the total power production of the island and 22% of the archipelago of the Azores.

In 2008, a numerical model of the Ribeira Grande geothermal reservoir was re-calibrated using up-to-date temperature, pressure, production and tracer test data. Forecasts of reservoir performance under several injection configurations were made, providing important information on how power production may be maximized, while minimizing the potential cooling impact caused by the return of injected water. Based on these forecasts, EDA Renováveis, S.A., decided to relocate the injection area in the Pico Vermelho sector, by drilling new injection wells farther from the production area.

The present work was developed under the scope of the final project for the Geothermal Training Programme of the United Nations University, in Iceland. An updated model of the temperature and pressure distribution in the Pico Vermelho sector of the Ribeira Grande geothermal field was developed based on warm-up temperature and pressure data from new wells PV9, PV10, PV11 and RG5, suggesting some continuity of the reservoir to the northeast, as previously indicated by AMT/MT surveys. A simulation and interpretation of the tracer test data conducted in the same sector of the field in 2007-2008, using the programs of the software package ICEBOX, is also part of this final project. The results show an overall strong hydraulic connection between the injection and production wells in this sector of the geothermal field.

1. INTRODUCTION

In Portugal, high-enthalpy geothermal resources can be found on the volcanic islands of Azores. The archipelago is situated in the North Atlantic Ocean, between latitudes 36°55′43″N and 39°43′23″N and

longitudes 24°46′15″W and 31°16′24″W, and comprises nine inhabited islands spread over a distance of 600 km. The Ribeira Grande geothermal field is located on São Miguel, the largest island of the archipelago, with a total area of 745 km^2 (Figure 1).

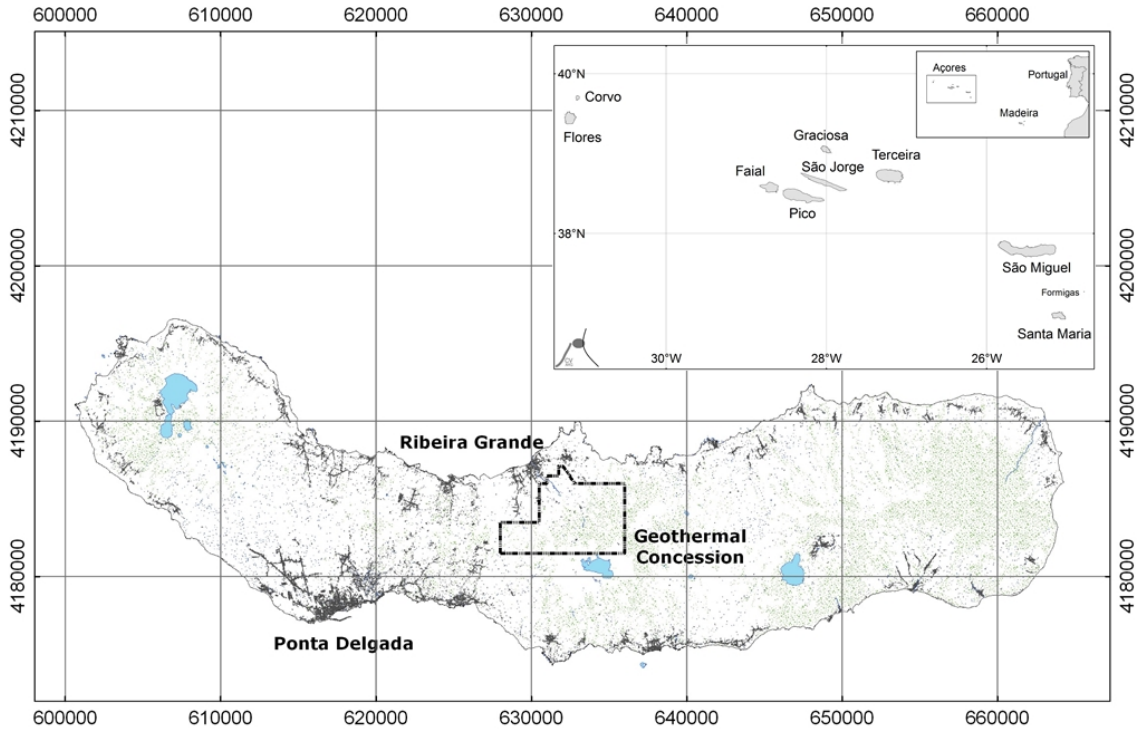

FIGURE 1: Geographic location of São Miguel Island (map provided by EDA Renováveis); map also shows the location of Ribeira Grande geothermal concession

The possible presence of high-enthalpy geothermal resources in the Azores became evident when, in 1973, geoscientists from Dalhousie University, while performing a deep drilling programme into the oceanic crust, decided to drill a research core-hole onshore, on São Miguel Island (north flank of Fogo volcano), intersecting formations with temperatures exceeding 200ºC at 550 m depth, while steam erupted from the hole when the drill string was removed (Muecke *et al.*, 1974). Since then, and until the late 1980s, several geological, geochemical and geophysical surveys were conducted in the Ribeira Grande geothermal field, the results of which have been used to interpret the conditions of the reservoir during development of the field.

These geological exploration activities led to the present scenario of exploitation of geothermal resources on São Miguel Island, where EDA Renováveis, S.A. (owned by EDA – Electricidade dos Açores, S.A., the electric power utility of the region), following the work of previous regional government institutions in the development of geothermal projects, operates two binary Organic Rankine Cycle power plants: Ribeira Grande and Pico Vermelho. The power plants have a combined capacity of 23 MW_e and are supplied by the geothermal fluid of deep wells drilled into the high-enthalpy, liquid-dominated Ribeira Grande geothermal reservoir. Figure 2 shows the location of the wells in the two sectors of the field: Cachaços-Lombadas and Pico Vermelho.

Nowadays, power production from geothermal resources represents about 43% of the electric consumption of the island of São Miguel and over 22% of the total demand of the archipelago. The need to meet the local government's policy of maximizing the use of clean, renewable and indigenous energy sources supports the expansion of geothermal projects in the Azores.

This paper was written under the scope of the final project of the six month geothermal training program of the United Nations University in Iceland and presents the results of the updated temperature and pressure distribution model of the Pico Vermelho sector of the Ribeira Grande geothermal field. A simulation and interpretation of tracer test data, collected in the same sector of the field in 2007-2008, is also part of this work.

2. RIBEIRA GRANDE GEOTHERMAL FIELD

2.1 General geological setting

The Azores islands stand astride the Mid-Atlantic Ridge following a NW-SE trend and emerge above the sea, in the North Atlantic Ocean, from a thick and irregular area of oceanic crust, roughly limited by the 2,000 m bathymetric curve (Azores Plateau). Some authors maintain that this structure is related to the presence of a deep mantle plume in the zone where the American, Eurasian and Nubian lithospheric plates meet at the "Azores Triple Junction" (Moore, 1990; Gaspar *et al.,* 2011).

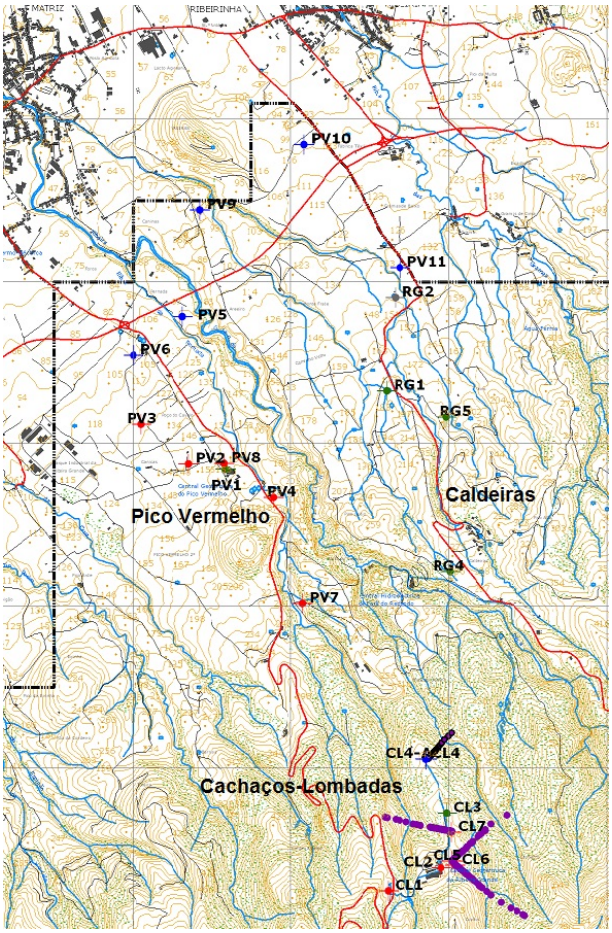

FIGURE 3: Surface map of the Ribeira Grande geothermal field showing location of wells (provided by EDA Renováveis)

Figure 3 shows the main tectonic features of the archipelago which are: in the west, the Mid-Atlantic Ridge (MAR); in the north, the North Azores Fracture Zone (NAFZ) and a complex alignment with a WNW-ESE direction, running from the MAR to the western limit of Gloria Fault (GF), designated as Terceira Rift (TR); in the South, the East Azores Fracture Zone (EAFZ). As a result of this complex geodynamic setting, seismic and volcanic activity is frequent in the region (Gaspar *et al.,* 2011).

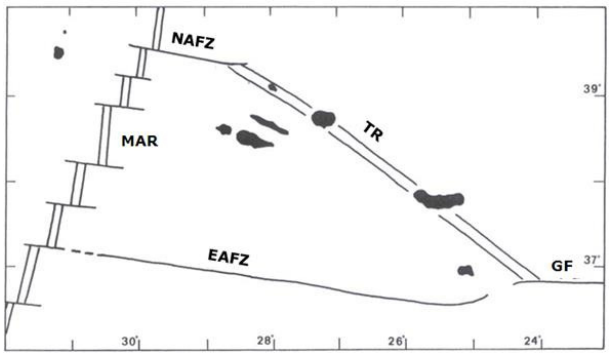

FIGURE 3: Main tectonic structures in Azores region (Gaspar, 1996)

The Ribeira Grande geothermal field is located on the north flank of the Fogo volcano, also known as Água de Pau Massif. Fogo volcano is located in the central part of the island of São Miguel, and is the largest of the three active central volcanoes of the island. The volcano rises to approximately 1,000 m and its summit caldera, with a lake occupying an area of 4.8 km^2, was formed as a result of numerous collapses and explosions, the most recent occurring during a sub-plinian eruption of 1563 followed by a basaltic flank eruption and the hydromagmatic explosive event of 1564 (Wallenstein *et al.*, 2007; Viveiros *et al.*, 2009; Moore, 1991).

The Fogo volcano is composed of a succession of trachytic to basaltic lava flows, trachytic domes, scoria cones, pyroclastic flows, lahars, pumice and ash deposits. Poorly exposed, the oldest deposits

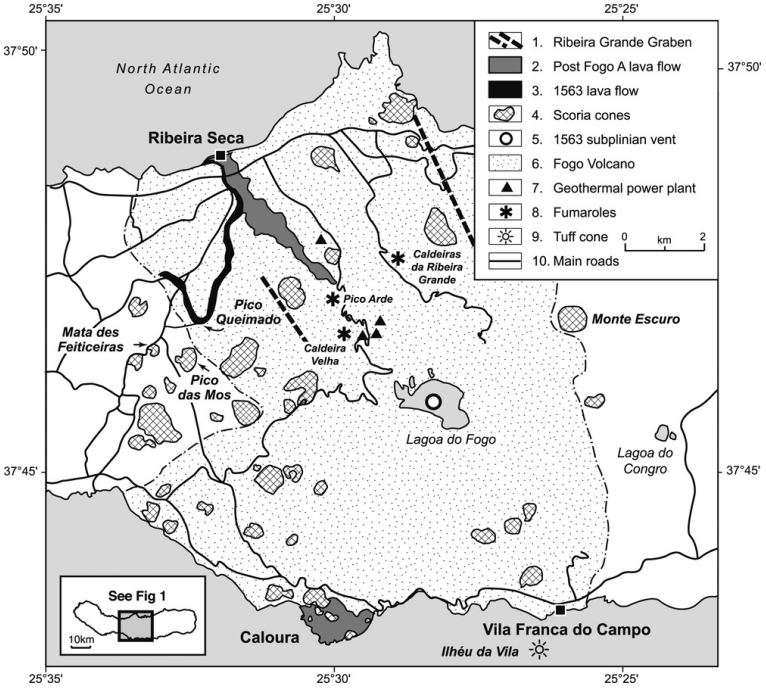

FIGURE 4: Morphostructural sketch of Fogo volcano (Wallenstein *et al.*, 2007)

date from more than 200,000 years ago (Figure 4) (Martini *et al.*, 2009; Wallenstein *et al.*, 2007). The northern flank of Fogo volcano is down-faulted by a NW-SE trending graben. It is also possible to observe NE-SW alignments and a circular system of faults, which might be responsible for the emplacement of trachytic domes on the upper part of the volcanic edifice (Silva *et al.*, 2012; Wallenstein *et al.*, 2007).

Several geothermal manifestations can be observed on this active central volcano, mainly on its northern flank, such as fumarolic fields, soil diffuse degassing areas, and thermal and CO_2 cold springs. Their locations are associated with the NW–SE fault system that defines the Ribeira Grande graben (Viveiros *et al.*, 2009).

2.2 Resume of the developmental history of the field

Ribeira Grande geothermal field was discovered through a research core-hole drilled in 1973 in Pico Vermelho area. Subsequent geological investigations conducted during 1975-1977 defined an extensive geothermal anomaly and, between 1978 and 1981, five exploratory wells were drilled in that area. In 1980, a 3 MW_e pilot plant based on a backpressure turbine from Mitsubishi was installed in Pico Vermelho sector, operating for 25 years.

In the southern sector of the field (Cachaços-Lombadas), a binary plant from Ormat (Ribeira Grande power plant) was installed in two phases: Phase A (5 MW_e) in 1994 and Phase B (8 MW_e) in 1998. Nowadays, the plant is supplied by the fluid from four geothermal wells and reinjection occurs through two injection wells. The total plant output is, on average, about 10 MW_e, less than the total capacity of the plant, due to insufficient fluid supply.

Meanwhile, in 2005, EDA Renováveis decided to proceed with further development of the Pico Vermelho sector, with the drilling of five new wells and replacement of the pilot plant with a new 10 MW_e binary plant. Due to the high productivity of the wells, Pico Vermelho power plant has a very flexible operation, needing only three of the five production wells available to provide the fluids needed for the plant.

2.3 Conceptual hydrogeological model

The Ribeira Grande geothermal field is an extensive, high-temperature geothermal system hosted by volcanic rocks (mainly a succession of trachytic to basaltic lavas and pyroclastic rocks) on the northern flank of the Fogo volcano. The geothermal reservoir is elongated in a northwest direction, and may have southwest and northwest boundaries that follow this trend, particularly at lower elevations. Up to the present, drilling has been insufficient to delineate the field's limits and the most

recent geoelectrical surveys indicate that it extends further to the northeast (GeothermEx, 2008; Ponte *et al.*, 2009; Pham *et al.,* 2010; Ponte *et al.*, 2010).

According to the conceptual hydrological model of the field, geothermal water with a maximum temperature of at least 250°C enters the reservoir in an upflow zone that is probably located in the southeast part of the field. The heat source for the hot water is presumably a body of magma or young intrusive rocks associated with the activity of Fogo volcano. According to isotopic analysis, the origin of the water is meteoric (GeothermEx, 2008; Ponte *et al.*, 2009; Pham *et al.,* 2010; Ponte *et al.*, 2010).

The principal flow direction into and within the reservoir at deeper levels is upward and to the northwest, following the northwest trend of faulting created by the regional tectonic setting, though there is probably some lateral flow toward the margins of the reservoir as well. At shallower levels (around -400 m elevation), a lateral, northwest flow appears to predominate over the upward flow, forming an extensive, relatively shallow reservoir in the Pico Vermelho sector (GeothermEx, 2008; Ponte *et al.*, 2009; Pham *et al.* 2010; Ponte *et al.*, 2010).

The permeability of the Ribeira Grande geothermal reservoir is associated with the fractures in the volcanic rocks of the Fogo volcano. Well data from the geothermal field indicate that a sequence of pyroclastic rocks altered to clay forms a relatively impermeable cap at the top of the reservoir. The lower limit of the reservoir (at least in the northwest, lower-elevation Pico Vermelho sector of the field) seems to be formed by impermeable clastic volcanic rocks at or near the transition zone between subaerial and submarine deposits (GeothermEx, 2008).

The chemical composition of the geothermal water is relatively homogeneous throughout the field, being mainly of a Na-Cl type with high HCO_3. Although the reservoir contains predominantly liquid water, boiling occurs and forms a steam or two-phase zone at the top of the reservoir in some sectors of the field. Progressive boiling of the reservoir water as it flows to the northwest reduces the content of non-condensable gases in the Pico Vermelho sector, compared with the Cachaços-Lombadas sector, although the difference is generally minor (GeothermEx, 2008).

2.4 Geophysical exploration

The first geophysical surveys in the Ribeira Grande geothermal field were conducted in the 1970s and 1980s, including DC resistivity and controlled-source audio-magnetotelluric surveys. They identified a well-defined geophysical anomaly that extends from the coastal area near the city of Ribeira Grande upward toward the summit of the volcano. In 2006, new audio-magnetotelluric and magnetotelluric surveys were conducted, identifying a large low-resistivity anomaly extending into the area northeast of the Pico Vermelho – Caldeiras, which is believed to be the result of hydrothermal alteration. In 2009-2010, this extension of the reservoir was partially confirmed by the drilling of new wells PV9, PV10, PV11, RG4 and RG5 (GeothermEx, 2008).

2.5 Numerical model predictions

In order to support the development of the northern area of the geothermal field, the conceptual model of the reservoir was updated and a numerical model was first developed in 2003. In 2008, the numerical model of the Ribeira Grande field was re-calibrated, using up-to-date temperature, pressure and production data from the geothermal wells, as well as tracer test data. The updated model was used to generate forecasts of reservoir performance under various possible injection configurations; this yielded important indications of how power production from the geothermal resource of the Ribeira Grande field may be maximized, while minimizing potential detrimental impacts caused by the return of injected water (GeothermEx, 2008).

According to the model calculations, continued injection into the existing injection wells of the Pico Vermelho sector could induce significant thermal breakthrough in all of the Pico Vermelho production wells, causing a reservoir temperature decline of about 50ºC over the next 30 years of production (GeothermEx, 2008).

Based on these forecasts, EDA Renováveis, S.A., decided to relocate the injection area in the Pico Vermelho sector. In 2009 and 2010, three new injection wells were drilled in the Pico Vermelho sector (PV9, PV10 and PV11) farther from the production area. In order to assess the area located northeast of Pico Vermelho, which was indicated by the previous AMT/MT results, exploration wells RG4 and RG5 were also drilled during the same drilling campaign.

3. ANALYSIS OF TEMPERATURE AND PRESSURE DATA

3.1 General concepts

Following the completion and testing of a geothermal well, either through injection or production, which give us the first estimates of well and reservoir properties, a period of warm-up is expected to occur for the well to recover in temperature after cooling was induced by circulation during drilling and cold water injection.

During the warm-up period, several temperature and pressure surveys are normally run and data is used to estimate the undisturbed reservoir temperature (formation temperature) and pressure, being essential for reservoir assessments of the geothermal resource, playing an essential role in the calibration of various reservoir models (Axelsson and Steingrímsson, 2012).

Convective processes outweigh conduction in geothermal systems as a means of heat transfer. Therefore, it is expected that wells with poor permeability heat up slowly, sometimes taking many months to completely stabilize, as the heating process is controlled by conduction, while permeable wells heat up more rapidly. The heat-up process is also dependent on the time-length of cooling during drilling, which is very variable (Grant and Bixley, 2011; Axelsson and Steingrímsson, 2012).

Commonly, for a long set of data, the Horner plot method is used for estimating the formation temperature. This method is a simple analytical method for analysing maximum bottom-hole temperatures to determine the formation temperature. The basic criteria for the technique is the straight-line relationship between the maximum bottom-hole temperature and ln(τ) with:

$$\tau = \frac{\Delta t}{\Delta t + t_0}, \tag{1}$$

where τ = Horner time,
Δt = The time passed since circulation stopped,
t_0 = The circulating time,

We see that:

$$\lim_{\Delta t \to \infty} \ln(\tau) = 0. \tag{2}$$

Considering the above and the fact that the system must have stabilized after infinite time, the maximum bottom-hole temperature is plotted as a function of ln (τ). Then, a straight line is drawn through the data and extrapolated to ln(τ)=0 to determine the formation temperature (Arason *et al.*, 2004). This method can also be applied to estimate the maximum temperature at a certain depth that has not been disturbed by cross-flow in the well.

The initial reservoir pressure, at a certain depth, is estimated through the intersection of several warm-up pressure profiles, which define the pressure pivot or pressure control point. If we consider a well with a single feed zone, the pressure in the well at the depth of this feed zone will be controlled by and become equal to the reservoir pressure. As the temperature of the wellbore fluid changes during the heating period, the density of the fluid also changes, but pressure at the feed zone is fixed by the reservoir pressure. Therefore, if a single feed-zone dominates a well, the pivot point defines the reservoir pressure at the feed-zone depth. If two, or more, feed-zones exist in a well, the pivot point defines average conditions instead (Grant and Bixley, 2011; Axelsson and Steingrímsson, 2012).

The reservoir pressure profile can't be measured directly in high-temperature wells. However, it can be estimated by hydrostatic extrapolation from the pivot point depth pressure value, using the formation temperature curve for the well to determine the water density as a function of depth. Estimating the reservoir pressure profile for all wells in the same field is important for understanding the pressure distribution in the reservoir (Steingrímsson, 2013).

3.2 Data from newly drilled wells

After drilling four new geothermal wells (PV9, PV10, PV11 and RG5 – see Figure 2), it was important to assess and update the information regarding the formation temperature and the initial reservoir pressure in the Pico Vermelho sector of the Ribeira Grande geothermal field. To do so, the warm-up temperature and pressure profiles were plotted along with the boiling point depth curve, against depth and elevation for each of the 10 geothermal wells of the Pico Vermelho sector. Afterwards, the formation temperature was estimated for the bottom-hole, as well as for other depths that have not been disturbed by cross-flow in the well, by using the software BERGHITI from the software package ICEBOX (Arason *et al.*, 2004). The Horner plot method was selected to determine the formation temperature. Figure 5 shows an example of a Horner plot for 500 m depth in the geothermal well PV11. After obtaining the formation temperature for several depths (preferably including the main feed zones), the formation temperature curve was drawn and plotted with the warm-up temperature profiles.

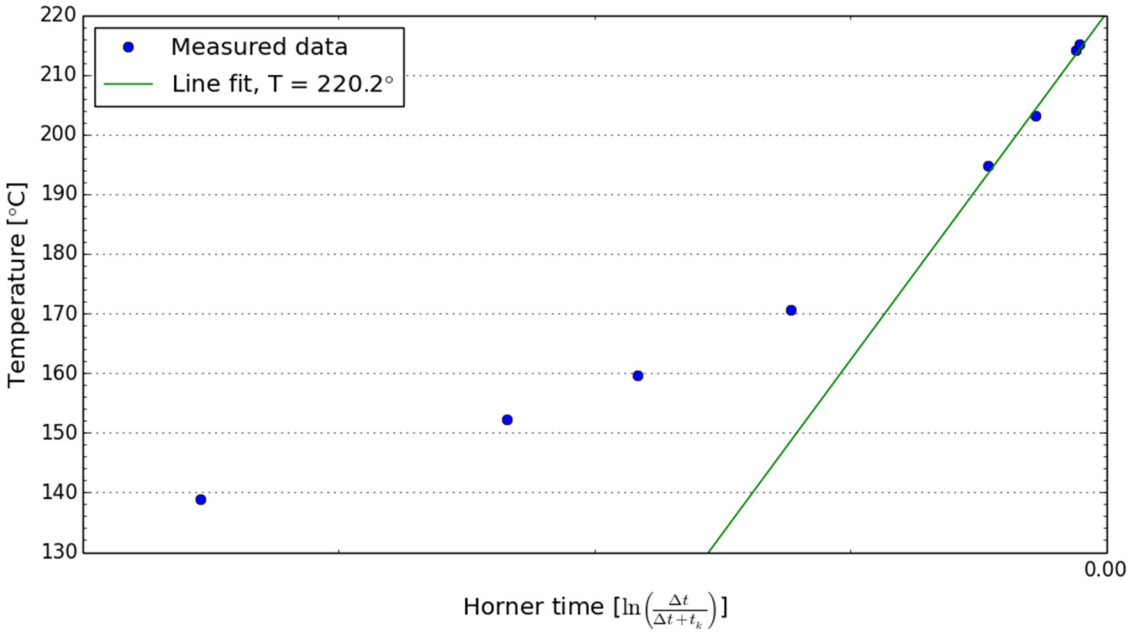

FIGURE 5: Horner plot for warm-up temperature data at 500 m depth in geothermal well PV11 (manual fitting)

For high-temperature wells, the boiling point depth curve (BPDC) is often plotted as a reference, as this curve defines the maximum possible formation temperature for the hydrothermal system, unless superheated conditions exist, which is an uncommon scenario (Steingrímsson, 2013).

To assess the initial reservoir pressure in that sector of the field, the software PREDYP from the software package ICEBOX (Arason *et al.*, 2004) was used. PREDYP computes pressure in a static water column for known temperatures and water levels (measured from wellhead) or wellhead pressure. The initial reservoir pressures were estimated for the same geothermal wells, considering the formation temperatures estimated previously. For each well, the reservoir pressure profile was adjusted to fit the most likely pressure pivot point of the well.

Figure 6 shows the warm-up temperature and pressure logs of the new geothermal wells PV9, PV10, PV11 and RG5, drilled in the northeast part of the Pico Vermelho sector along with the estimated formation temperature conditions and initial pressure. The temperature and pressure profiles, as well as the estimated formation temperature and initial pressure of the other Pico Vermelho geothermal wells, are presented in Appendix I.

Analysing Figure 6, we can verify that the water temperature is below the boiling point at all depths, with the exception of the last three logs of well RG5, indicating that, during the warm-up, some boiling might have taken place in the upper part of the well. Geothermal well PV9 seems to intersect the top of the reservoir between 300 and 400 m depth, and from that depth to around 600 m, the isothermal profile of the temperature logs indicates that convection is the dominant heat transfer process within the formation. At that depth, we can observe a temperature reversal, most likely associated with the total loss that occurred during drilling at 621 m depth (circulation was never regained while drilling the rest of the well). From that depth, which is probably the main feed zone of the well, to the well-bottom, well PV9 appears to have penetrated a permeable zone or multiple zones. The interval between 600 m and the bottom of the well took longer to warm-up, probably due to the fact that it stood in contact with the drilling fluid (cold fluid) for a longer time. The maximum formation temperature was estimated as 226.3ºC at 600 m depth. The initial reservoir pressure is estimated to be 48.6 bar at the same depth.

Analysing the behaviour of the temperature profiles made during the warm-up period of well PV10, we verify that probably the survey made on November 30th should reflect the true formation temperature, as the well probably had reached thermal equilibrium. Therefore, formation temperatures increase rapidly with depth from the surface to about 350 m depth, probably while intersecting the caprock of the reservoir. Then, the top of reservoir seems to be intersected, as a gradual increase in temperature is observed, reaching a maximum of about 201°C at 500 m depth. A slight temperature reversal occurs, with temperatures declining to about 185°C at the bottom of the well. A pivot point is difficult to define in well PV10, however we can assume one at 500 m depth, where pressure is 39 bar. The behaviour of the temperature profiles in well PV10, with no indication of important feed zones, suggests that the well penetrates a peripheral zone of the Ribeira Grande reservoir in the Pico Vermelho sector of the field, probably near an outflow zone.

The geothermal well PV11 appears to have penetrated the reservoir near 400 m depth, with a possible inflow to the well at around 450 m. Formation temperatures reach 229.3°C at that depth. The initial reservoir pressure is estimated to be 39.3 bar at the same depth, where a pressure control point can be identified. The zone below the major loss zone (near 465 m) remained substantially cooled by drilling, when compared with the bottom of the well where permeability might be limited.

Well RG5 is located in the northeastern-most part of the field. From the analysis of temperature and pressure logs made during the warm-up period, it is reasonable to consider that the last temperature profile made on October 18th, 2010, reflects nearly stabilized conditions. The maximum formation temperature estimated is 229.4°C at 800 m depth. The initial reservoir pressure is estimated to be 52.3 bar at the same depth.

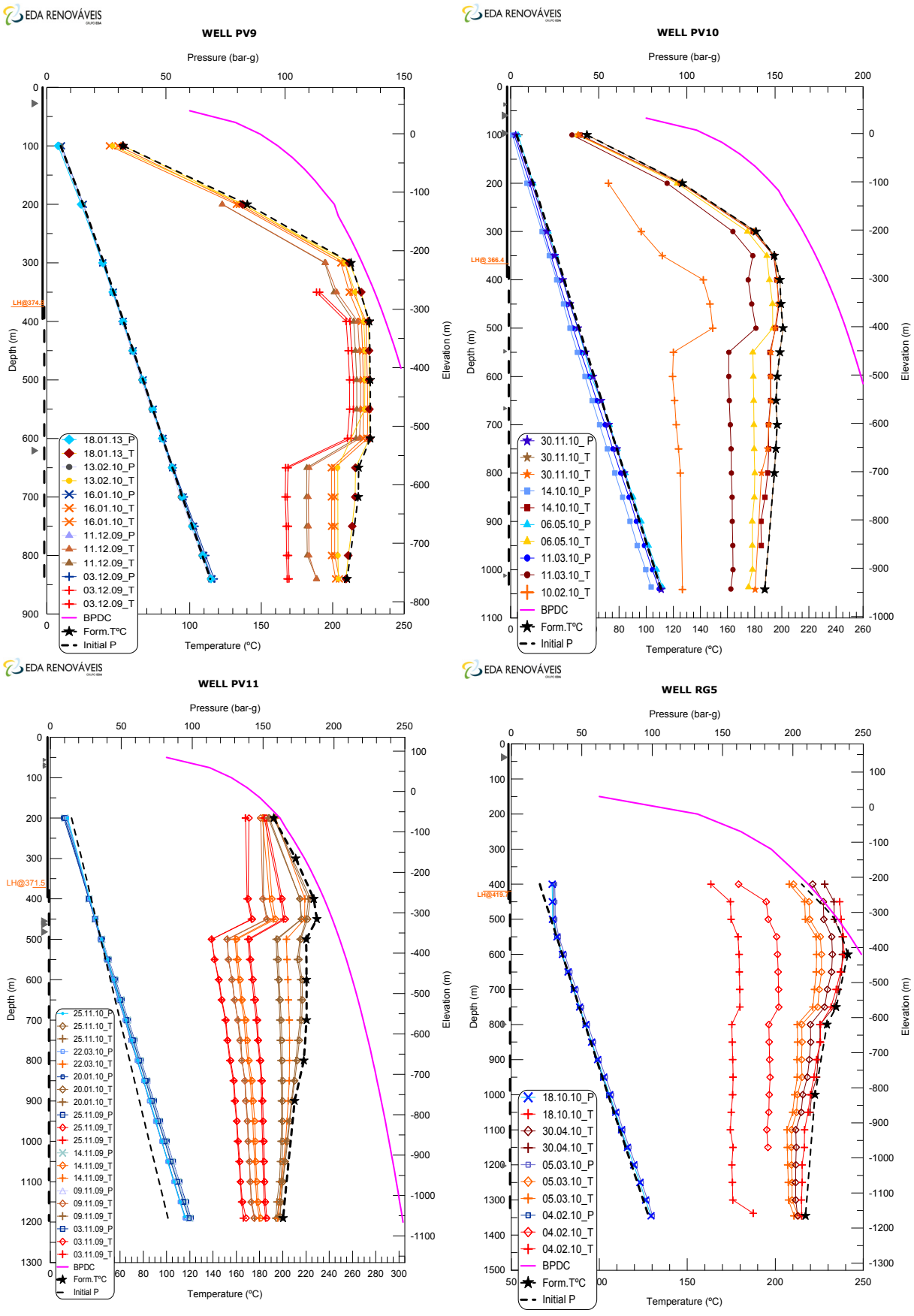

FIGURE 6: Warm-up temperature and pressure logs, as well as estimated formation temperature and initial reservoir pressure for geothermal wells PV9, PV10, PV11 and RG5

Formation temperature and initial reservoir pressure profiles were gathered and plotted as a function of elevation, both for new wells and for the other wells in Pico Vermelho (Figure 7). When comparing the formation temperatures estimated from the new wells drilled in Pico Vermelho (Figure 7A), we observe that well RG5 presents the highest temperatures (maximum temperature of about 241ºC at 420 m b.s.l.) and well PV10 the lowest ones. This observation seems to be in accordance with the conceptual model of the Ribeira Grande geothermal field, where it is considered that the geothermal fluid, with a maximum temperature of at least 250°C, enters the reservoir through an upflow zone, probably located in the southeast part of the field (to the east of the wells in the Cachaços-Lombadas area) and flows laterally at shallower levels to the northwest, forming an extensive and relatively shallow reservoir in the Pico Vermelho sector. In Figure 7B, the formation temperature profiles estimated from wells PV2, PV4, PV7 and PV8 show that these wells are located in a permeable high-temperature reservoir zone (maximum temperature of about 245ºC at 470 m b.s.l. in well PV4). Wells PV3 and PV5 present the lowest temperatures. Overall, in Pico Vermelho sector, the highest temperatures observed were between 200 m b.s.l. and 600 m b.s.l. Reservoir temperature and

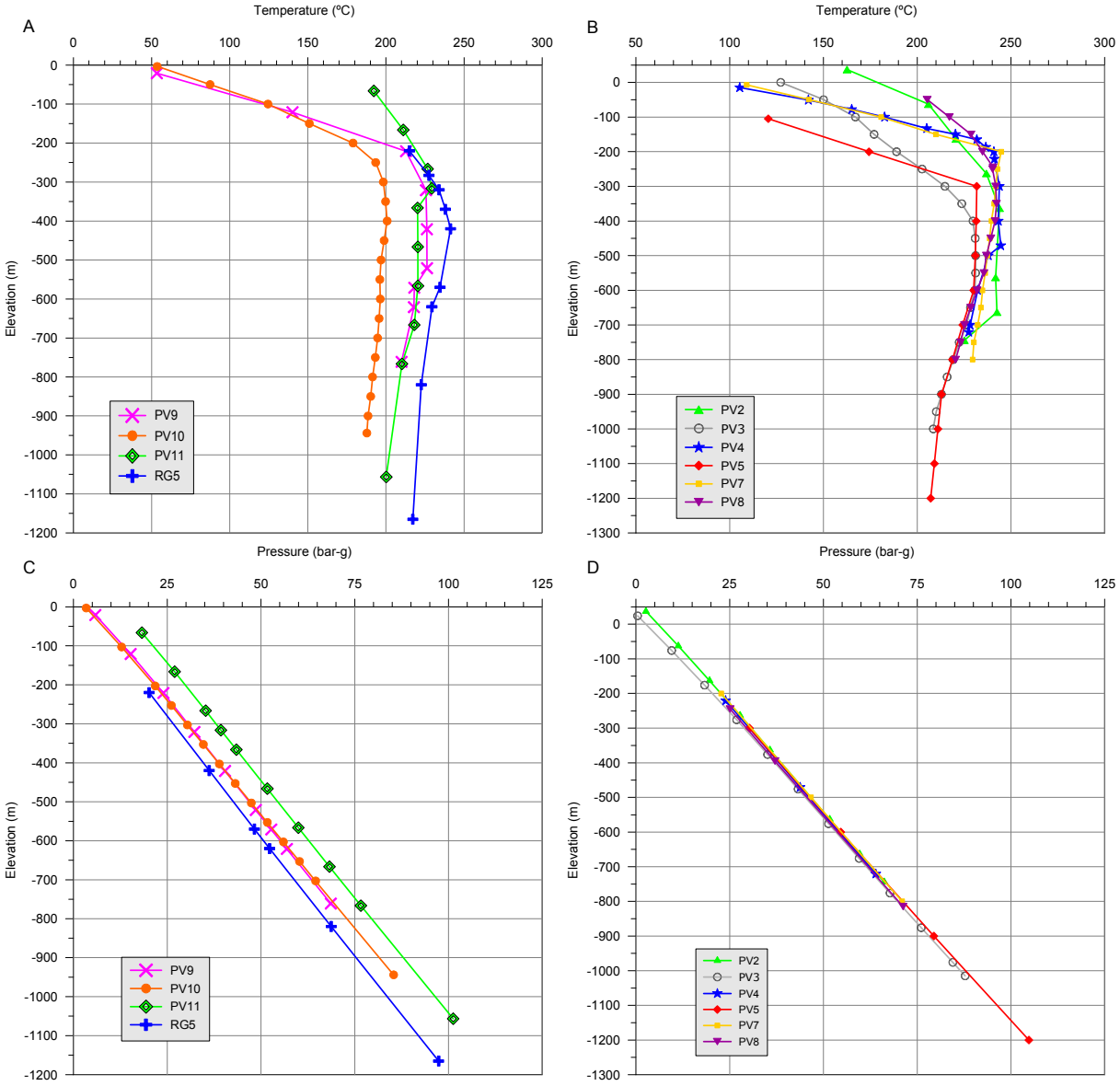

FIGURE 7: Formation temperatures profiles (A and B) and initial reservoir pressure profiles (C and D) estimated for the geothermal wells in the Pico Vermelho sector

permeability in the northwest part of the field, in the vicinity of wells PV3, PV5 and PV10, seem to be lower. Figure 7D shows a consistent initial reservoir pressure in the area of the older wells in Pico Vermelho (PV2 to PV8), while to the west the pressure seems to be lower around well RG5 and higher around well PV11 (Figure 7C). One possible interpretation of this variation can be related with the depth and permeability of the main feed-zones of the wells.

3.3 Temperature and pressure models

Based on the estimated formation temperature and initial pressure of the reservoir in the Pico Vermelho sector, temperature and pressure contour maps were drawn in order to show their distribution in this sector of the geothermal field. Figure 8 shows temperature contour maps, made at 200 m intervals, from 200 to 800 m b.s.l.

From the analysis of the temperature distribution in Figure 8, we note that at 200 m b.s.l., a zone of higher temperatures is present in the area of wells PV4, PV7 and PV8. At -400 m, temperatures are nearly isothermal over a significant distance in the SE-NW direction, slightly decreasing towards well PV10 (north-northeast). The 600 m b.s.l. map shows a temperature distribution with a similar pattern to the one at -400 m, but temperature has started to decrease. By 800 m b.s.l., the overall decrease in temperature of the Pico Vermelho sector indicates that the reservoir lies mainly above this level, where temperatures remain approximately isothermal. By incorporating the data from the new geothermal wells into the model, we verify that there is no sign of the existence of a boundary between them and the other wells, indicating a continuous reservoir in the overall Pico Vermelho sector. Furthermore, the newly drilled wells show no indication of a reservoir boundary in the eastern part of the geothermal field, which agrees with the results of the AMT/MT surveys.

Figure 9 shows the initial reservoir pressure contour maps at 200 m intervals, from 200 to 800 m b.s.l. Initial pressure conditions are often more difficult to estimate accurately than formation temperature, due to varying influential factors, and such contour maps are more difficult to interpret. From the analysis of the pressure distribution in Pico Vermelho sector, we observe that the pressure is higher in north and west part of the field, declining to the east, in the vicinity of well RG5. Thus, the pressure distribution pattern is somewhat the opposite of the temperature distribution, which can be explained by the fact that the pressure gradient is controlled by fluid density, which varies with temperature. Another condition to consider is the role of the main feed zones that are controlling the pressure distribution.

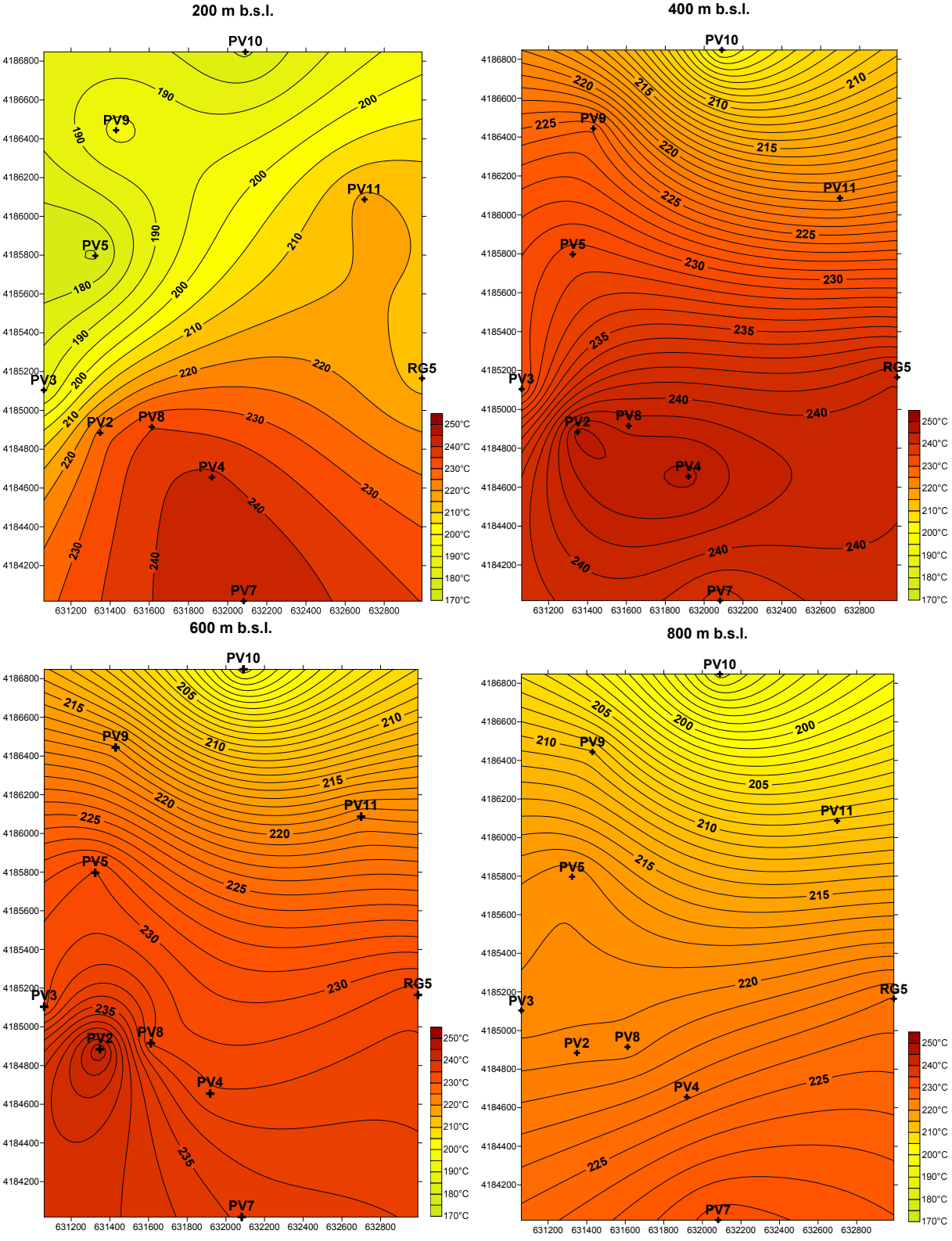

FIGURE 8: Contour maps of formation temperature at four different elevations (200, 400, 600 and 800 m b.s.l.)

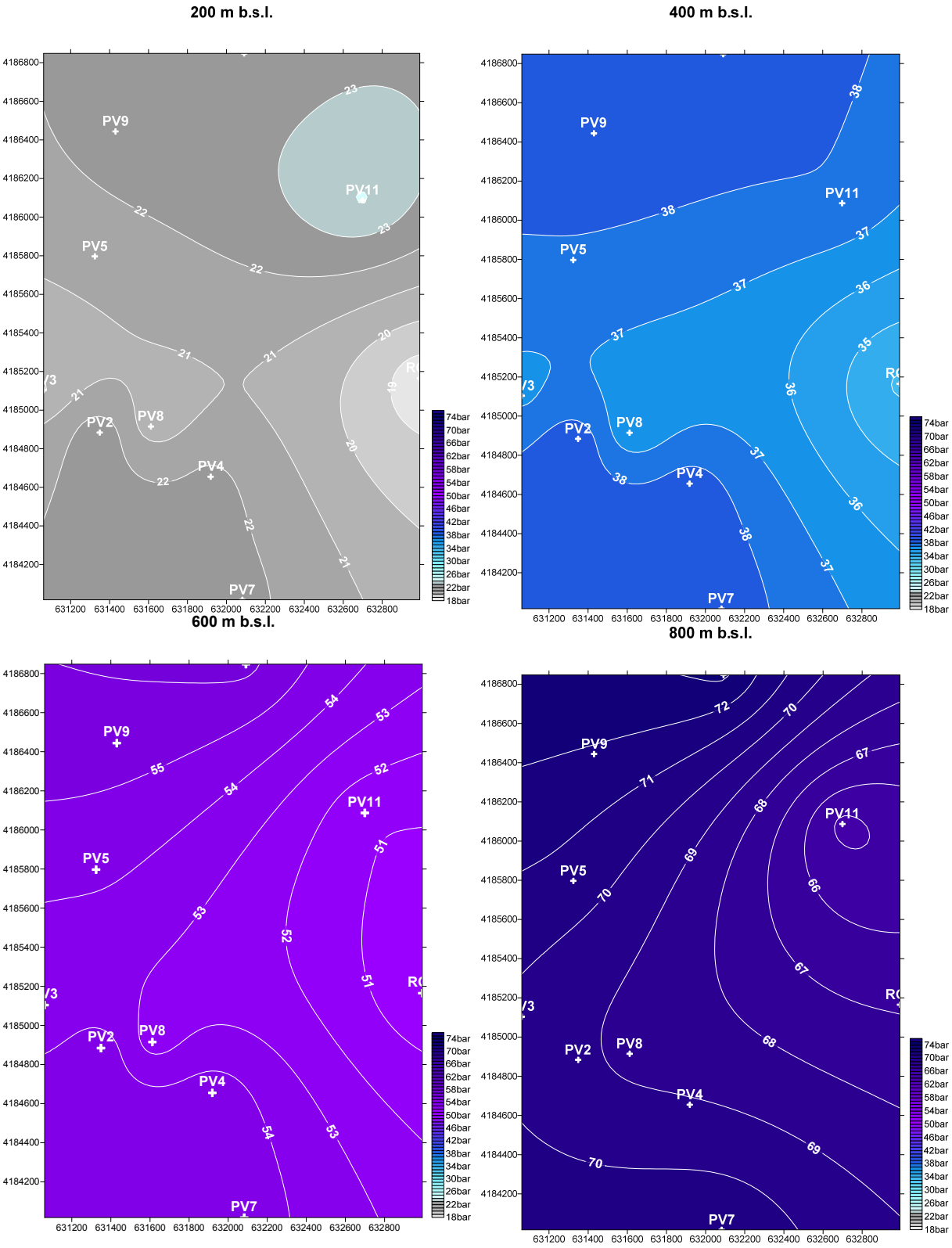

FIGURE 9: Contour maps of initial reservoir pressure at four different elevations (200, 400, 600 and 800 m b.s.l.)

4. ANALYSIS OF TRACER TEST DATA

4.1 Reinjection

One of the most important and challenging tasks of sustainable management of geothermal resources is related to the reinjection of the geothermal fluid after heat conversion into electricity at the power plants. Mass extraction during long-term production causes a pressure draw-down inside the geothermal reservoir. Through reinjection, additional recharge is provided to the reservoir and, as a result, the necessary pressure support is restored. Reinjection also enhances thermal extraction from reservoir rocks along flow-paths. The production potential of geothermal systems is mainly determined by pressure decline caused by mass extraction, but also by energy content. Pressure declines with time in closed systems or ones with limited recharge and, therefore, production potential is rather limited by lack of water than lack of energy (Axelsson *et al.*, 2005).

From the environmental point of view, reinjection is a proper option for the disposal of the geothermal fluid from power plants, contributing also to minimizing the surface subsidence caused by production induced pressure decline (Axelsson, 2012; Axelsson *et al.*, 2005). Nevertheless, there are some disadvantages associated with reinjection, namely the possible cooling of production wells, or cold-front breakthrough, often because of "short-circuiting" along direct flow-paths such as open fractures between the injection wells and the production area of the geothermal field. The proper equilibrium between providing the right pressure support to the reservoir and avoiding the cooling of the production wells is one of the most challenging tasks in the management of geothermal resources.

In order to evaluate the impact of reinjection on the decline of temperature in production wells, tracer tests are a powerful tool in geothermal management studies. According to Axelsson (2012), tracer tests provide information on the nature and properties of the flow-paths that connect injection and production wells and control the rate of cooling during long-term reinjection. The importance of tracer tests lies in the fact that the thermal breakthrough time (beginning of cooling) is usually several orders of magnitude greater (2 to 4) than the tracer breakthrough time, conferring tracer tests a predictive power.

The models used to interpret geothermal tracer test data are based on the theory of solute transport in porous and fractured hydrological systems, which includes transport by advection, mechanical dispersion and molecular diffusion (Axelsson *et al.*, 2005).

4.2 Tracer test in the Pico Vermelho sector

The exploitation scheme of geothermal resources in the Ribeira Grande geothermal field comprises the reinjection of all the geothermal fluid after heat conversion into electricity in the power plants.

In order to evaluate the overall hydraulic connection in the Ribeira Grande geothermal reservoir, a tracer test was conducted between October 2007 and May 2008. The test consisted of injecting three different types of naphthalene disulfonate tracers (1,6-NDS, 2,6-NDS and 2,7-NDS) into injection wells PV6, PV5, and CL4, respectively. Routine sampling for analysis of tracer returns was conducted from production wells CL1, CL2, CL5, PV2, PV3, and PV4 over a period of eight months. For the purpose of this work, we will only refer to the data from the Pico Vermelho sector (Pham *et al.*, 2010). The analysed tracer return data were used to further calibrate the numerical reservoir model. The results showed a rapid and relatively large magnitude return of the tracer injected into well PV6 in wells PV2, PV3 and PV4, indicating that well PV6 injection can have a detrimental effect on the fluid production temperature of these production wells. It could also be anticipated that well PV8 could also be negatively impacted by injection into well PV6, because this well is close to wells PV2 and PV4. Injection into well PV5 also indicated a negative impact on the temperature of the produced fluid of the Pico Vermelho wells, but to a lesser degree than well PV6. The tracer injected into well CL4, in

the southern part of the field (Cachaços-Lombadas sector), was not detected in the Pico Vermelho sector (Figure 10) (Pham *et al.*, 2010).

Under the current scheme of exploitation, the numerical model predicted that injection into wells PV5 and PV6 will cause significant cooling of the reservoir in the Pico Vermelho sector, at a rate of about 1.7°C per year (Pham *et al.*, 2010).

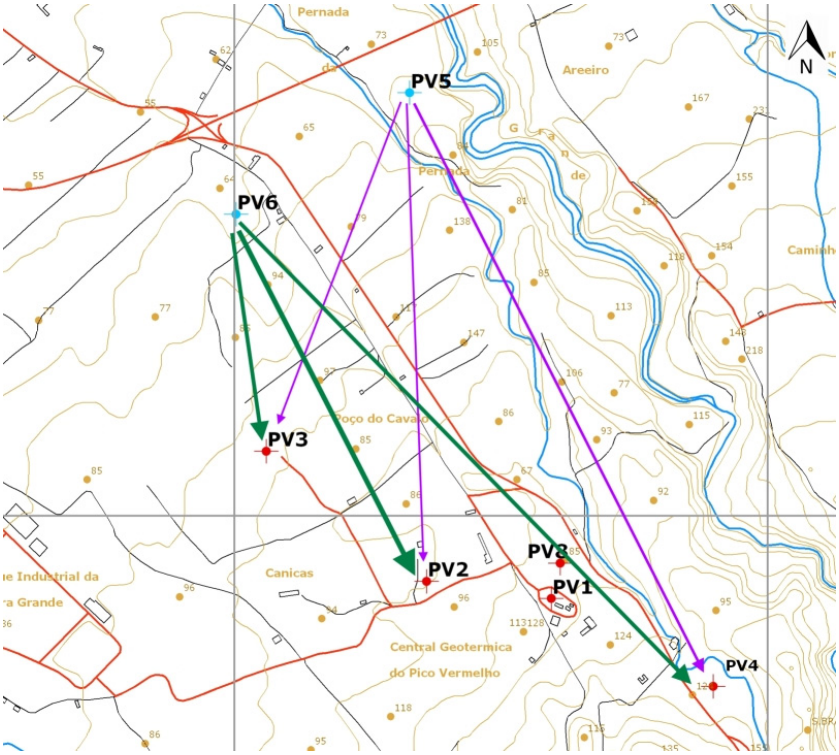

FIGURE 10: Tracer return pattern in Pico Vermelho sector (EDA Renováveis)

For the purpose of the present work, the data from the tracer test conducted in 2007-2008 in Pico Vermelho sector was analysed using the programs related to tracer test analysis and reinjection simulation, which are included in the software package ICEBOX (Arason *et al.*, 2004), taught at the Geothermal Training Programme of the United Nations University.

4.2.1 Tracer mass recovery

During tracer test analysis, the first step is to estimate the mass of tracer recovered during the test. Such an estimate is reached thorough the following equation:

$$m_i(t) = \int_0^t C_i(s) Q_i(s) ds \tag{3}$$

where $m_i(t)$ = Cumulative mass recovered in production well number i (kg), as a function of time;
C_i = Tracer concentration (kg/L or kg/kg);
Q_i = Production rate of well number i (L/s or kg/s).

The program TRMASS was used for this purpose. However, when the tracer sampling is carried out for a long period of time, considerably longer than the tracer breakthrough time, it is necessary to correct the tracer recovery for the amount of tracer which is recirculating in the system, due to the secondary return of tracer that was produced in the production wells and reinjected back into the reservoir. We can observe this effect through a relatively high concentration of tracer along the tail of the recovery curve, which causes the decrease of the slope of the tail of the curve. The program TRCORRC was used to correct that effect on the recovery curve. The results are presented in Figures 11–13.

Considering the average brine production rate of each of wells PV2, PV3 and PV4 during the tracer test and that 100 kg of each tracer were dissolved in 1 m^3 of fresh water, the parameters related with the amount of tracer recovered for each pair of wells are summarized in Table 1.

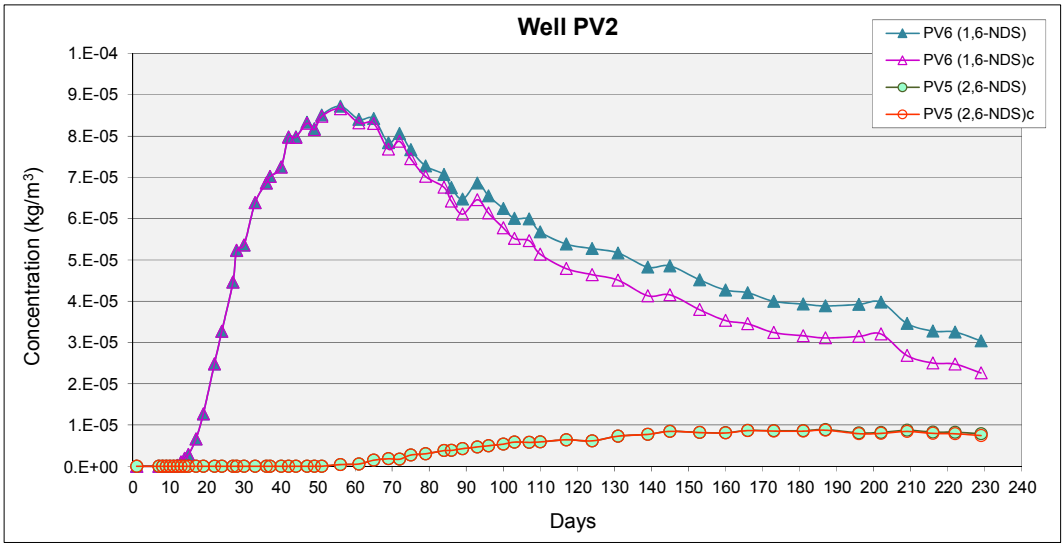

FIGURE 11: Adjusted (corrected for tracer recirculation) tracer recovery curves for well PV2

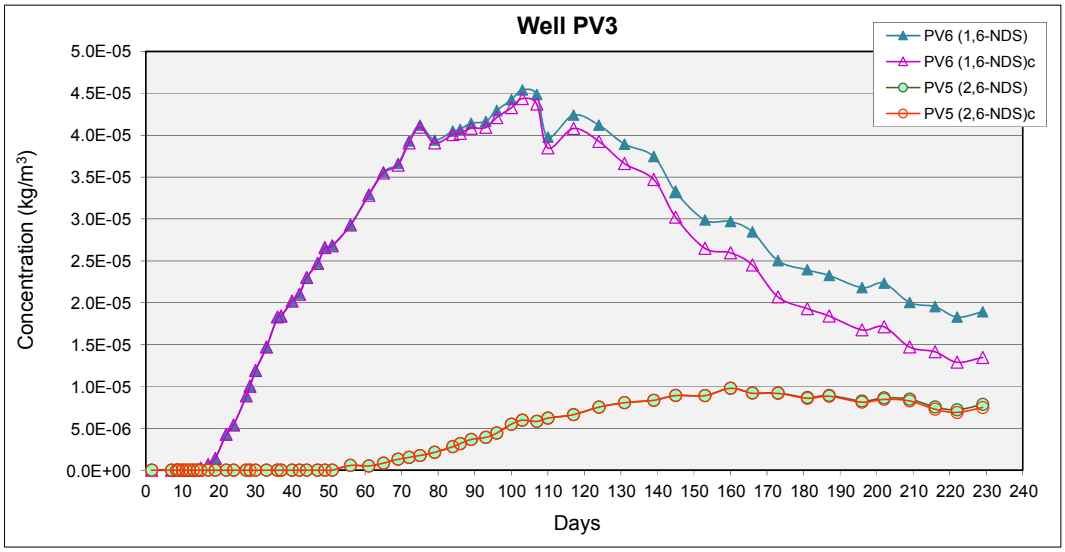

FIGURE 12: Adjusted (corrected for tracer recirculation) tracer recovery curves for well PV3

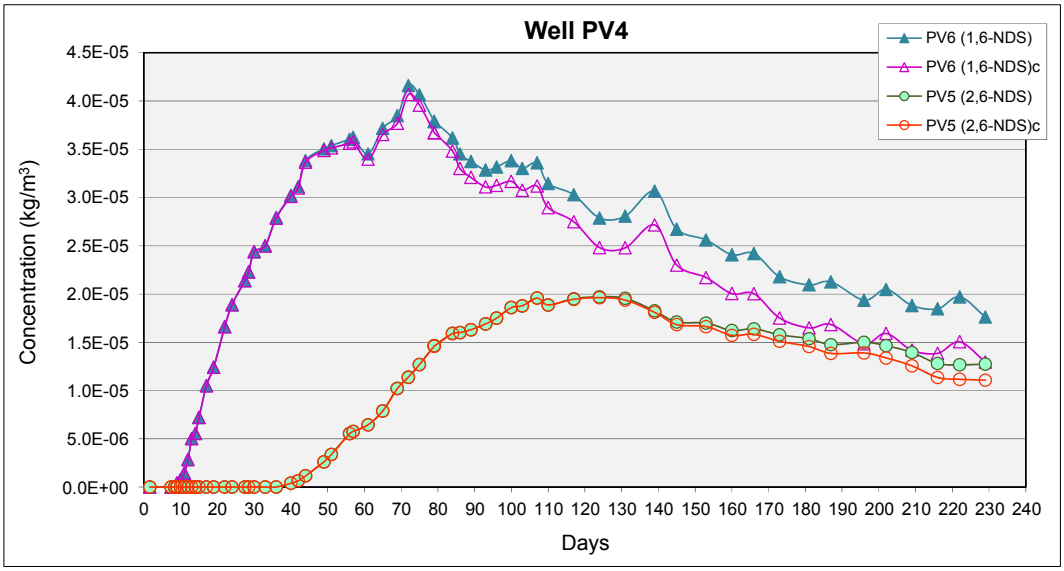

FIGURE 13: Adjusted (corrected for tracer recirculation) tracer recovery curves for well PV4

TABLE 1: Mass recovery results for geothermal production wells PV2, PV3 and PV4

Injection-production well pair	Maximum concentration (kg/m^3)	Tracer breakthrough time (days)	Mass recovery (%)
PV6-PV2	8.7x10^{-5}	12	25.06
PV6-PV3	4.4x10^{-5}	15	15.78
PV6-PV4	4.1x10^{-5}	9	18.28
PV5-PV2	8.7x10^{-6}	56	2.71
PV5-PV3	9.8x10^{-6}	56	3.16
PV5-PV4	1.9x10^{-5}	40	9.14

The results presented above suggest that injection well PV6 and production well PV2 have a strong hydraulic connection, since the 1,6-NDS tracer took only 12 days to first appear in the production well and the peak amount was about 8.7x10^{-5} kg/m^3 (87 ppb). The connection between well PV6 and production wells PV3 and PV4 is also significant; however, the amount of tracer return is less than that observed in well PV2.

The returns of the 2,6-NDS tracer, injected into well PV5, show that this injection well has a weaker hydraulic connection with production wells PV2, PV3 and PV4, when compared with well PV6. This tracer had a significant return in well PV4 with a maximum concentration of 1.9x10^{-5} kg/m^3, with a first arrival after 40 days.

4.2.2 Simulation and interpretation of data

During a first stage assessment, tracer test interpretation can be based on simple models, as presented by Axelsson *et al.* (2005). They describe a one-dimensional flow-channel model, where it is assumed that the flow between injection and production wells may be approximated by one-dimensional flow in flow-channels. According to the same authors, these channels may be parts of near-vertical fracture-zones or parts of horizontal interbeds or layers. The channels may be envisioned as being delineated by the boundaries of these structures, on one hand, and flow-field stream-lines, on the other. In other cases, these channels may have larger volumes involved in the flow between wells. In some cases more than one channel may be assumed to connect an injection well and a production well, for example connecting different feed-zones in the wells involved.

The mathematical equations that are the basis of the interpretation method for tracer tests are related to the differential equation for solute (chemical substance dissolved in fluid) transport, simplified for the case of one-dimensional flow (Equation 4):

$$D\frac{\partial^2 C}{\partial x^2} = u\frac{\partial C}{\partial x} + \frac{\partial C}{\partial t} \tag{4}$$

where D = Dispersion coefficient (m^2/s), given by $D = \alpha_L u$;
C = Tracer concentration in the flow-channel (kg/m^3);
x = Distance along the flow channel (m);
u = Average fluid velocity in the channel (m/s), given by: $u = q/\rho A\emptyset$, with q the injection flow through the channel (kg/s); ρ the water density (kg/m^3); A the average cross-sectional area of the flow channel (m^2) and $\emptyset$ the flow channel porosity (%).

Because molecular diffusion is neglected in this simple model, and assuming an instantaneous injection of a mass of tracer at time zero, as well as conservation of the tracer according to $c \cdot Q = C \cdot q$, the solution to Equation 4 is given by:

$$c(t) = \frac{uM\rho}{Q}\frac{1}{2\sqrt{\pi Dt}}e^{-(x-ut)^2/4Dt} \tag{5}$$

where $c(t)$ = Tracer concentration in the production well fluid;
Q = Production rate (kg/s);
M = Mass of tracer injected at time t= 0 (kg).

The results of the simulation give important information on the flow channel cross-sectional area (Aø) and dispersivity (α_L), as well as the mass of tracer recovered through a given channel, which is equal to, or less than, the mass of tracer injected. In the case of two or more flow-channels, the analysis gives an estimate of these parameters for each channel. Through the estimates of a flow channel cross-sectional area, the flow channel pore space volume ($xA\emptyset$) can be estimated (Axelsson *et al.*, 2005).

The program TRINV simulates the tracer test data through inversion. A model with one or more flow-channels is defined by the user, and a first estimate of the model parameters is obtained. This DOS-mode program uses non-linear least-squares fitting to simulate the data and obtain the model properties, i.e. the flow channel volume, dispersivity (α_L) and tracer mass recovered (Mr). In addition to the distance between wells (along a flow channel) and volume of flow-paths, mechanical dispersion is the only mechanism assumed to control the tracer return curves in the method presented above. The model does not consider molecular diffusion, i.e., the delay of the tracers by diffusion from the flow-paths into the rock matrix, which causes the tracer to diffuse into the rock matrix when the tracer concentration in the flow path is high and vice-versa. Some authors claim that this effect can be negligible in fractured rock except when fracture apertures are small, flow velocities are low and rock porosity is high (Axelsson *et al.*, 2005).

It should be emphasised that many other models have been developed to simulate geothermal tracer tests. It is often possible to simulate a given dataset by more than one model; therefore, a specific model may not be uniquely validated (Axelsson *et al.*, 2005).

Considering the above, the tracer recovery curves were simulated for production wells PV2, PV3 and PV4 (Figures 14-16), and the principal results of the interpretation are presented in Table 2.

TABLE 2: Model parameters used to simulate tracer recovery for wells PV2, PV3 and PV4

Injection-production well-pair	Channel	Flow path distance x (m)	Flow velocity u (m/s)	Cross-sectional area AØ (m^2)	Estimated volume $xA\emptyset$ (m^3)	Dispersivity (α_L) (m)	Mass recovery (%)
PV6-PV2	1	759	1.6×10^{-4}	32	24288	110	13.5
	2	1138.5	7.8×10^{-5}	101	114988	239	20.4
PV6-PV3	1	717	7.9×10^{-5}	82	58794	191	16.9
	2	1075.5	1.1×10^{-4}	8	8604	42	2.3
PV6-PV4	1	1331	1.6×10^{-4}	56	74536	555	24
PV5-PV2	1	904	5.1×10^{-5}	155	140120	144	5.7
PV5-PV3	1	770	4.9×10^{-5}	146	112420	79	5.1
PV5-PV4	1	1260	7.5×10^{-5}	202	254520	179	10.8
	2	1890	2.2×10^{-4}	23	43470	127	3.5

The flow path distance between each well pair was defined by calculating the distance between the most likely feed zones of the wells. For injection wells PV5 and PV6, the main feed zones were assumed to be located at -550 m and -950 m, respectively. For well pairs PV6-PV2, PV6-PV3 and PV5-PV4, two channels were required for the above simulation, assuming for the second flow channel a longer length (e.g. due to sinking of the colder, and denser, injection fluid to a greater depth before it ascends to the production feed-zone), corresponding to an addition of 50% of the length of the main flow channel. For every well pair, determinate coefficients of 99.5 to 99.7% were achieved, with the exception of well-pair PV6-PV4, with 98.6%, showing a very good match between the simulated curves and the measured tracer concentrations that were recovered in the production wells.

From the analysis of the model parameters, it is verified that the 1,6-NDS tracer that was injected into well PV6 was recovered at a higher percentage in the production wells than the 2,6-NDS tracer which was injected into well PV5, suggesting that the first injection well has a stronger connection with the production area of Pico Vermelho than injection well PV5. The greatest mass recovery percentage is observed for well pair PV6-PV2 (approx. 34%) and the lowest, about 5%, was observed for well pair PV5-PV3. If we consider the dispersivity, we verify that there is some heterogeneity in the results obtained. Great dispersivity is normally associated with heterogeneous flowpaths, which could be associated, for example, with a network of fractures controlling the flow, rather than just a single fracture. Results of Table 2 were used to calculate cooling predictions for the three production wells.

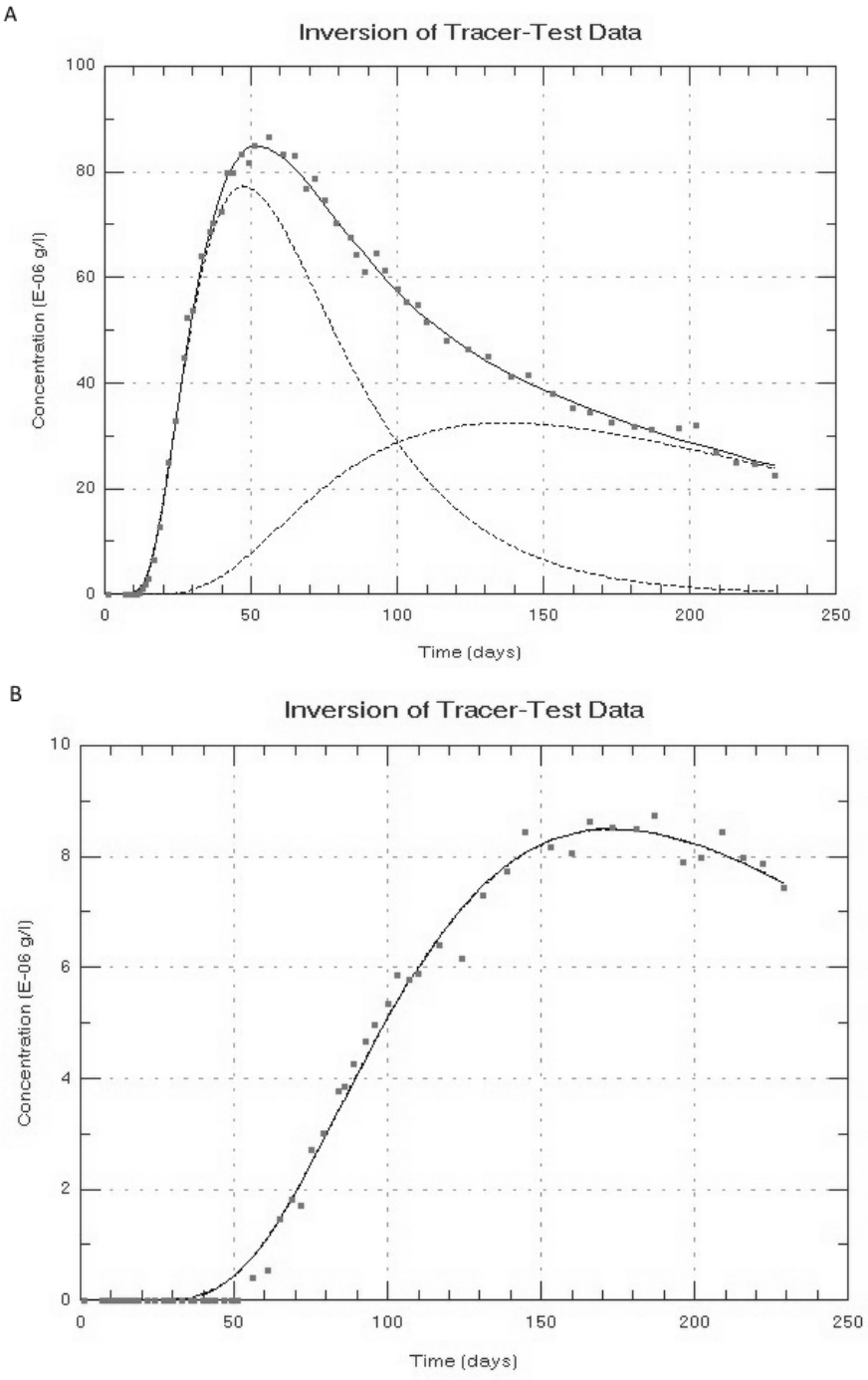

FIGURE 14: Observed (squares) and simulated tracer recovery curves for well PV2; A) Recovery of tracer 1,6-NDS (injected into well PV6); B) Recovery of tracer 2,6-NDS (injected into well PV5)

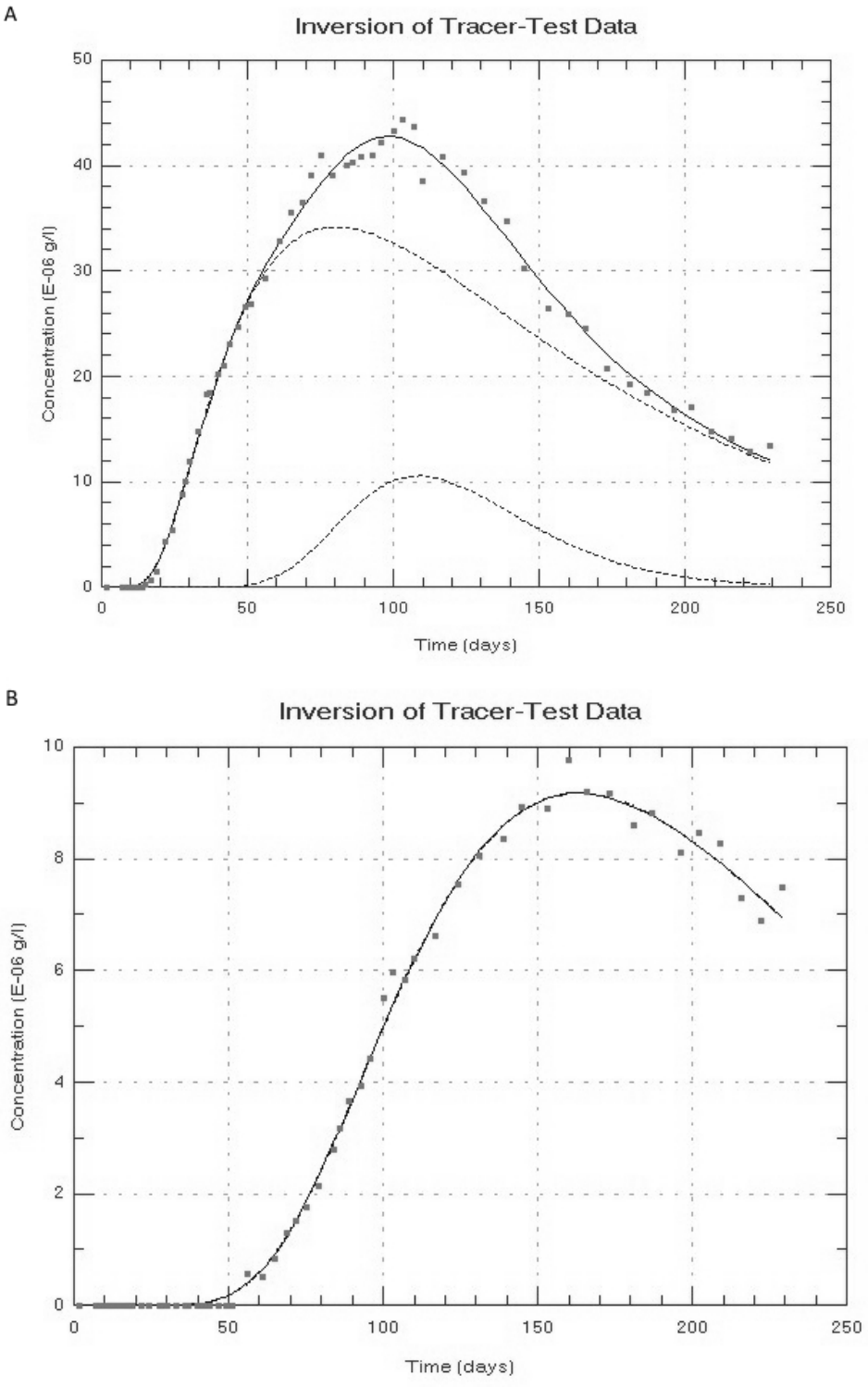

FIGURE 15: Observed (squares) and simulated tracer recovery curves for well PV3; A) Recovery of tracer 1,6-NDS (injected into well PV6); B) Recovery of tracer 2,6-NDS (injected into well PV5)

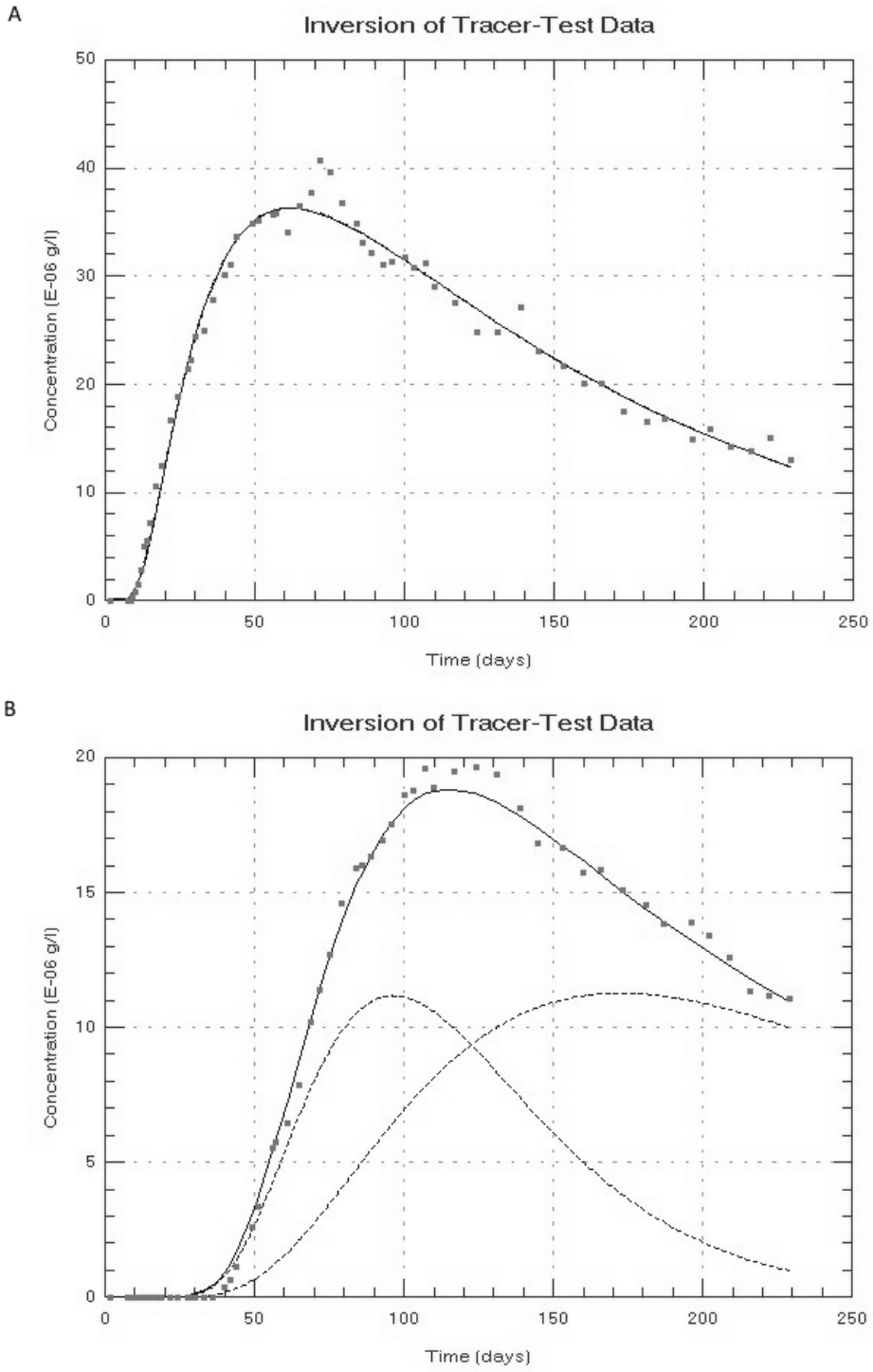

FIGURE 16: Observed (squares) and simulated tracer recovery curves for well PV4; A) Recovery of tracer 1,6-NDS (injected into well PV6); B) Recovery of tracer 2,6-NDS (injected into well PV5)

4.2.3 Prediction of temperature decline during long-term production

Temperature decline during long-term reinjection (thermal breakthrough) is not only determined by the volume of the flow-channel(s) involved, but also by the surface area and porosity of the flow-channel(s), as a large surface area flow channel leads to slow cooling and vice-versa. Therefore, it is important to have additional information on the flow-path properties/geometry or to make some

assumptions on those. Additional data, as temperature changes, or data on chemical variations should not be neglected as constraints for cooling predictions (Axelsson *et al.*, 2005).

The mathematical equations giving the response of the model for cooling predictions are:

$$T(t) = T_0 - \frac{q}{Q}(T_0 - T_i)\left[1 - erf\left\{\frac{kxh}{c_w q\sqrt{\kappa(t - x/\beta)}}\right\}\right] \quad (6)$$

$$\beta = \frac{qc_w}{(\langle\rho c\rangle_f hb)} \qquad \text{with} \qquad \langle\rho c\rangle_f = \rho_w c_w \phi + \rho_r c_r (1 - \phi) \quad (7)$$

where $T(t)$ = Production temperature (ºC);
T_0 = Initial reservoir temperature (ºC);
T_i = Injection temperature (ºC);
q = Injection flow-rate in each flow channel (kg/s);
Q = Production rate (kg/s);
x = Distance between injection and production wells (m);
k = Thermal conductivity of reservoir rock;
κ = Thermal diffusivity of rock (m^2/s), given by $k/\rho c_p$, with k its thermal conductivity; ρ its density (kg/m^3) and c_p its specific heat capacity (J/kg ºC);
ρ and c are density and heat capacity of water (w) and rock (r);
h and b are height and width of a flow path (m);
ϕ = flow path porosity (%).

Cooling predictions should be calculated considering two extremes regarding flow-channel dimensions: a small surface area, or pipe-like flow channel, which can be considered a pessimistic model with minimal heat transfer (rapid cooling); and a large surface area flow channel, such as a thin fracture-zone or thin horizontal layer, which can be considered an optimistic model with effective heat transfer (slow cooling).

Considering the scheme of reinjection for the Pico Vermelho power plant, at the time the tracer test was conducted (using wells PV5 and PV6 as injection wells with a total flow of around 145 kg/s of geothermal fluid), the program TRCOOL was used to calculate the theoretical temperature decline for production wells PV2, PV3 and PV4, for a period of 30 years, while considering both scenarios presented above.

The model parameters used for the cooling predictions for wells PV2, PV3 and PV4 can be found in Table 3. A pessimistic scenario was assumed, where the ratio between height (h) and width (b) of the flow channels was given by h=5b and also an optimistic scenario, where that ratio was given by h=100b. For all cases, an average porosity of 15% was assumed for the predictions. The results of the cooling predictions are presented in Figure 17.

The cooling predictions indicate, for an optimistic scenario for well PV2, a temperature decline of about 22.5ºC in 30 years and about 64ºC for a pessimistic scenario. Regarding well PV3, we verify that the prediction for the same time period is less severe than for well PV2, with a drop in temperature of about 6ºC, considering the optimistic scenario and around 38.6ºC considering a more pessimistic scenario. Well PV4 is also strongly affected by cooling, with a temperature decline of about 20ºC predicted for the optimistic scenario, and around 55ºC considering the pessimistic scenario, for the same time period of 30 years.

When plotting the monitoring temperature data of wells PV2, PV3 and PV4 (represented as dots in Figure 17) together with the cooling predictions, between 2007 and 2014, we verify that: the pessimistic scenarios are unlikely, and that actually the observed data are close to being in-between the optimistic and pessimistic predictions. But if the injection into wells PV5 and PV6 is maintained for a

period of 30 years, it is not unlikely that the temperature in well PV2 will decline about 41ºC (± 21ºC) and around 35ºC (± 15ºC) in well PV4. Regarding production well PV3, the prediction of a significant decline in the temperature is more uncertain, as the well has been recovering its initial temperature. This increase of the measured temperature in well PV3 in the last couple of years is probably due to the fact that this well has not been producing on a continuous basis for the power plant and, therefore, has been to a large extent kept closed. In Pico Vermelho sector there is an excess of fluid production which allows a very flexible operation, requiring only three production wells to saturate the power plant (10 MW).

Although the model parameters used in 2007-2008 by GeothermEx (2008) to perform the cooling predictions are unknown, namely the geometry of the flow channel(s) and respective volume(s), we see that the results, obtained through the tracer test analysis presented here, are in general comparable with the ones predicted previously by GeothermEx, with a temperature decline of around 1.4ºC per year for well PV2 and 1.2ºC per year for well PV4. GeothermEx (2008) predicted an overall temperature decline of 50ºC for the Pico Vermelho sector, which can also be compared with the predictions in Figure 17.

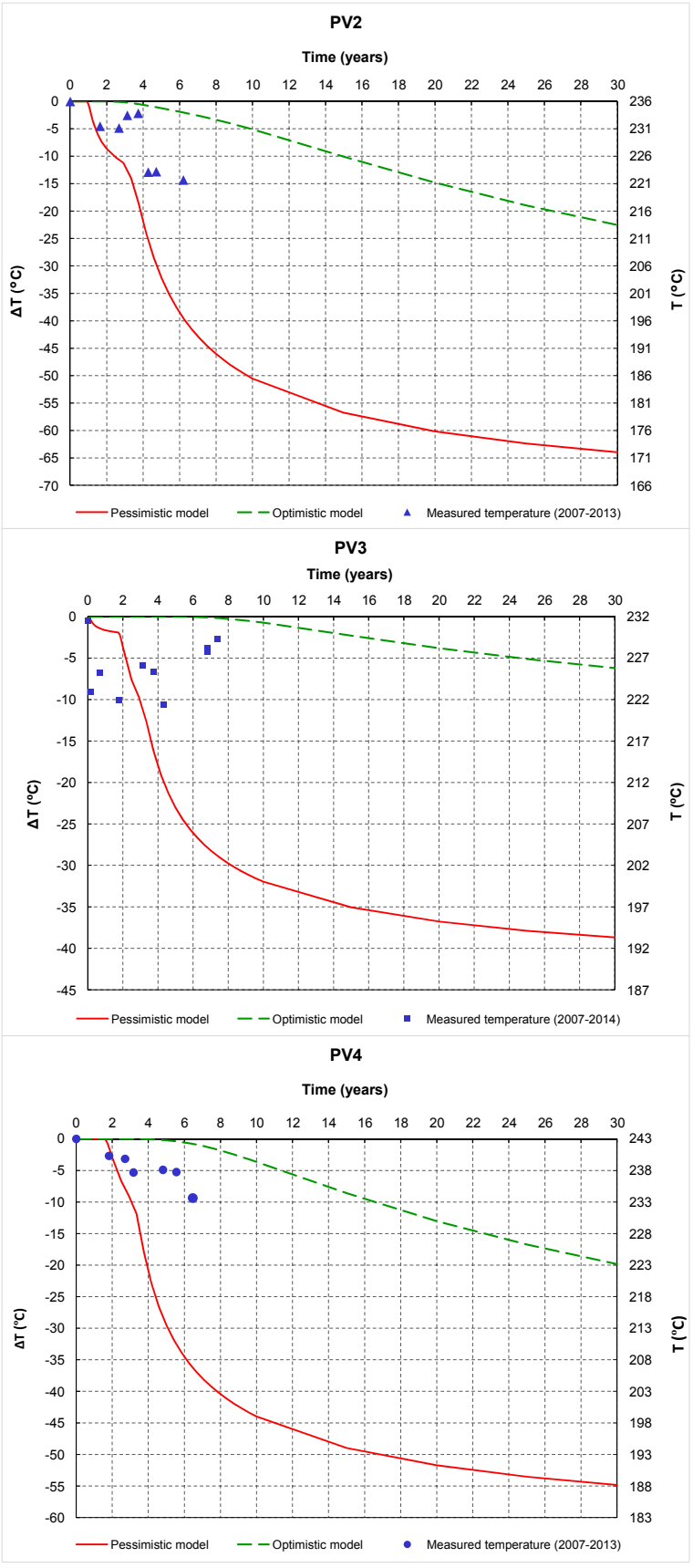

FIGURE 17: Cooling predictions for production wells PV2, PV3 and PV4, considering a period of 30 years

TABLE 3: Model parameters used for the cooling predictions for wells PV2, PV3 and PV4

Injection-production well-pair	Scenario	Channel	Flow channel distance x (m)	Flow channel width/thickness b (m)	Flow channel height/extent h (m)
PV6-PV2	Pessimistic	1	759	6.6	32.9
		2	1138.5	11.6	58
	Optimistic	1	759	1.5	150
		2	1138.5	2.6	260
PV5-PV2	Pessimistic	1	904	14.4	72
	Optimistic			3.2	320
PV6-PV3	Pessimistic	1	717	10.5	52.3
		2	1075.5	0.5	2.5
	Optimistic	1	717	2.3	234
		2	1075.5	0.1	110
PV5-PV3	Pessimistic	1	770	14	69.7
	Optimistic			3.1	311.6
PV6-PV4	Pessimistic	1	1331	8.6	43.2
	Optimistic			1.9	193
PV5-PV4	Pessimistic	1	1260	16.4	82
		2	1890	5.5	27.6
	Optimistic	1	1260	3.7	370
		2	1890	1.2	123.6

5. CONCLUSIONS

The Ribeira Grande geothermal field is a high-temperature, liquid-dominated system, hosted by volcanic rocks, mainly a succession of trachytic to basaltic lava flows and pyroclastic flows. The heat source of the reservoir is presumably a body of magma or young intrusive rock associated with the activity of the Fogo volcano and the origin of the water is meteoric. The system seems to be controlled by the NW faulting trend created by the regional tectonic setting. Well data indicate that a sequence of pyroclastic rocks, altered to clay, form a relatively impermeable cap at the top of the reservoir.

In order to estimate the formation temperature and initial reservoir pressure in the Pico Vermelho sector of the Ribeira Grande geothermal system, the warm-up temperature and pressure profiles of new wells PV9, PV10, PV11 and RG5 were analysed together with the warm-up temperature and pressure profiles of the other Pico Vermelho wells. Based on the estimated formation temperature and initial pressure of the reservoir, temperature and pressure contour maps were drawn in order to show their distribution in this sector of the field.

By incorporating the data from the new geothermal wells into the temperature model, we verify that the reservoir in Pico Vermelho lies mostly between the 200 and 800 m b.s.l. and there is no evidence of the existence of a boundary between the wells located to the west and the new ones located to the east, indicating a continuous reservoir in the overall Pico Vermelho sector.

In order to evaluate the overall hydraulic connection in the Ribeira Grande geothermal reservoir, a tracer test was conducted between October 2007 and May 2008**.** For the purpose of the present work, the data from the tracer test was analysed using the programs related to tracer test analysis and reinjection simulation which is included in the ICEBOX software package (TRCORRC, TRMASS, TRINV and TRCOOL). The results suggest a strong hydraulic connection between injection wells PV5 and PV6 and the production area in Pico Vermelho, as was previously predicted.

Cooling predictions based on the results of the tracer recovery modelling indicate, for an optimistic scenario in well PV2, a temperature decline of about 22.5ºC in 30 years and about 64ºC for a pessimistic scenario. Regarding well PV3, we verify that the prediction for the same time period is less severe than for well PV2, with a drop in temperature of about 6ºC, considering the optimistic scenario and around 38.6ºC considering the more pessimistic scenario. Well PV4 is also strongly affected by cooling, with a predicted temperature decline of about 20ºC for an optimistic scenario and around 55ºC considering a pessimistic scenario, for the same time period of 30 years. After comparing actual temperature monitoring for wells PV2, PV3 and PV4, we verify that the pessimistic scenarios are unlikely, but if injection into wells PV5 and PV6 is maintained for a period of 30 years, it is considered likely that the temperature in well PV2 will decline about 41ºC (± 21ºC) and around 35ºC (± 15ºC) in well PV4. The prediction for production well PV3 is uncertain, since the well has been recovering its initial temperature, possibly due to the fact that this well has been kept closed for the last couple of years.

ACKNOWLEDGEMENTS

I would like to address my acknowledgments to Mr. Lúdvík S. Georgsson, director of the Geothermal Training Programme of the United Nations University (UNU-GTP), as well as to all the technical staff of UNU-GTP, namely Mr. Ingimar G. Haraldsson, Ms. María Gudjónsdóttir, Ms. Málfrídur Ómarsdóttir, Ms. Thórhildur Ísberg and Mr. Markús A.G. Wilde for the kind support provided during the training in Iceland. Sincere thanks to Dr. Gudni Axelsson and Ms. Saeunn Halldórsdóttir, from ÍSOR, for the supervision and guidance during the preparation of the present project.

A special word of appreciation is addressed to EDA Renováveis, S.A., for the support given during the training in Iceland and for allowing the use of the Ribeira Grande geothermal field data for the purpose of the present work.

REFERENCES

Arason, T., Björnsson, G., Axelsson, G., Bjarnason, J., and Helgason, P., 2004: *ICEBOX – Geothermal reservoir engineering software for Windows, a user's manual*. ÍSOR, Reykjavík, report ISOR-2004/014, 80 pp.

Axelsson, G., 2012: Role and management of geothermal reinjection. *Proceedings of the Short Course on Geothermal Development and Geothermal Wells, organized by UNU-GTP and LaGeo, Santa Tecla, El Salvador,* 22 pp.

Axelsson, G. and Steingrímsson, B., 2012: Logging, testing and monitoring geothermal wells. *Proceedings of the Short Course on Geothermal Development and Geothermal Wells, organized by UNU-GTP and LaGeo, Santa Tecla, El Salvador*, 20 pp.

Axelsson, G., Björnsson, G., and Montalvo, F., 2005: Quantitative interpretation of tracer test data. *Proceedings of the World Geothermal Congress 2005, Antalya, Turkey*, 12 pp.

Gaspar, J.L., 1996: *Ilha Graciosa (Açores): Volcanological history and assessment of hazards*. University of the Açores, Azores, PhD thesis (in Portuguese), 256 pp.

Gaspar, J.L., Queiroz, G., Ferreira, T., Amaral, P., Viveiros, F., Marques, R., Silva, C., and Wallenstein, N., 2011: *Geological hazards and monitoring at the Azores (Portugal)*. Articles, Disaster

Management Theme, Earth Observation (*www.earthzine.org/2011/04/12/geological-hazards-and-monitoring-at-the-azores-portugal/).*

GeothermEx, Inc., 2008: *Update of the conceptual and numerical model of the Ribeira Grande geothermal reservoir, São Miguel, Açores*. Report for SOGEO – Sociedade Geotérmica dos Açores, S.A.

Grant, M.A. and Bixley, P.F., 2011: *Geothermal reservoir engineering* (2nd ed.). Academic Press, NY, 359 pp.

Martini, F., Bean, C., Saccorotti, G., Viveiros, F., and Wallenstein, N., 2009: Seasonal cycles of seismic velocity variations detected using coda wave interferometry at Fogo volcano, São Miguel, Azores, during 2003-2004. *J. Volcanology & Geothermal Res.,181,* 231-246.

Moore, R., 1990: Volcanic geology and eruption frequency S. Miguel, Azores. *Bull. Volcanol. 52*, 602–614.

Moore, R., 1991: Geology of three late Quaternary stratovolcanoes on São Miguel, Azores. *USGS Bull. 1990,* 1-26.

Muecke, G.K., Ade-Hall, J.M., Aumento, F., McDonald, A., Reynolds, P.H., Hyndman, R.D., Quintino, J., Opdyke, N., and Lowrie, W., 1974: Deep drilling in an active geothermal area in the Azores. *Nature 252 (5481),* 281–285.

Pham, M., Klein, C., Ponte, C., Cabeças, R., Martins, R., and Rangel, G., 2010: Production/injection optimization using numerical modeling at Ribeira Grande, São Miguel, Azores, Portugal. *Proceedings of the World Geothermal Congress 2010, Bali, Indonesia*, 6 pp.

Ponte, C., Cabeças, R., Martins, R., Rangel, G., Pham, M., and Klein, C., 2009: Numerical modeling for resource management at Ribeira Grande, São Miguel, Azores, Portugal. *Geothermal Resources Council, Trans., 33,* 847-853.

Ponte, C., Cabeças, R., Rangel, G., Martins, R., Klein, C. and Pham, M., 2010: Conceptual modeling and tracer testing at Ribeira Grande, São Miguel, Azores, Portugal. *Proceedings of the World Geothermal Congress 2010, Bali, Indonesia*, 11 pp.

Silva, R., Havskov, J., Bean, C., and Wallenstein, N., 2012: Seismic swarms, fault plane solutions, and stress tensors for São Miguel Island central region (Azores). *J. Seismol., 9-1*, 21 pp.

Steingrímsson, B., 2013: Geothermal well logging: temperature and pressure logs. *Presented at* "*Short Course V on Conceptual Modelling of Geothermal Systems", organized by UNU-GTP and LaGeo, Santa Tecla, El Salvador*, 16 pp.

Viveiros, F., Ferreira, T., Silva, C., Óskarsson, N., and Hipólito, R. 2009: *Natural and anthropogenic influences on the gas geochemical monitoring at Fogo Volcano (São Miguel Island, Azores).* VOLUME project, EU PF6 (No. 018471), 299-308.

Wallenstein, N., Duncan, A.M., Chester, D.K., and Marques, R., 2007: Fogo Volcano (São Miguel, Azores): a hazardous edifice. *Géomorphologie: Relief, Processes, Environment, 3*, 259-270.

APPENDIX I: Warm-up temperature and pressure logs, as well as estimated formation temperature and initial reservoir pressure for geothermal wells PV2, PV3, PV4, PV5, PV7 and PV8

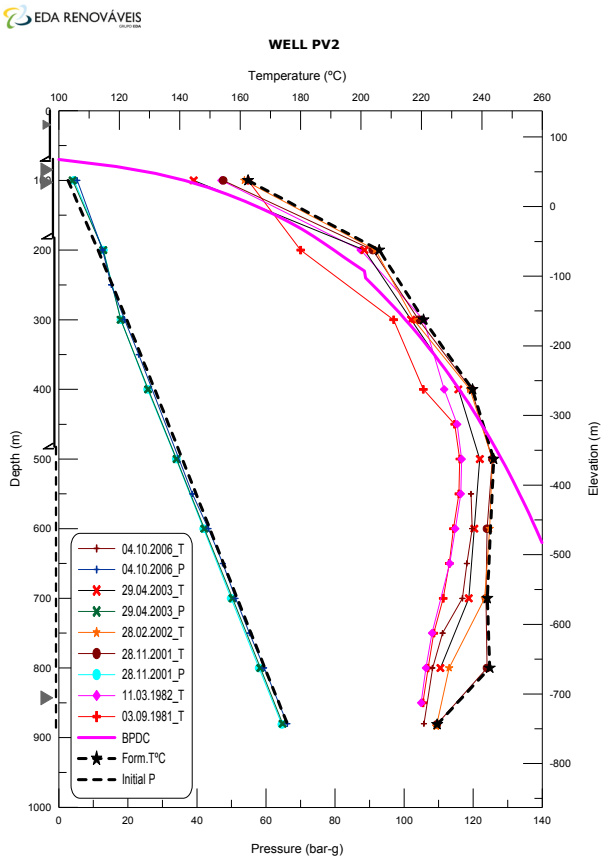

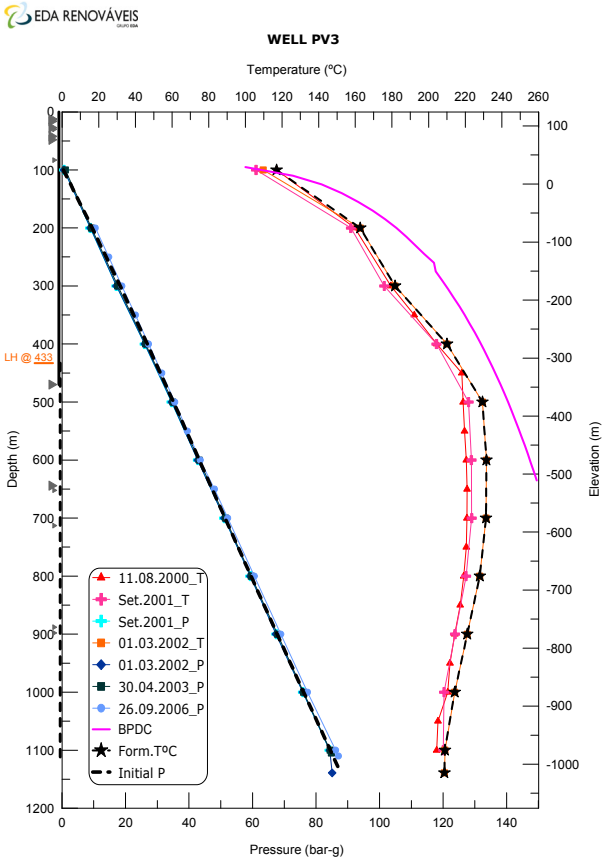

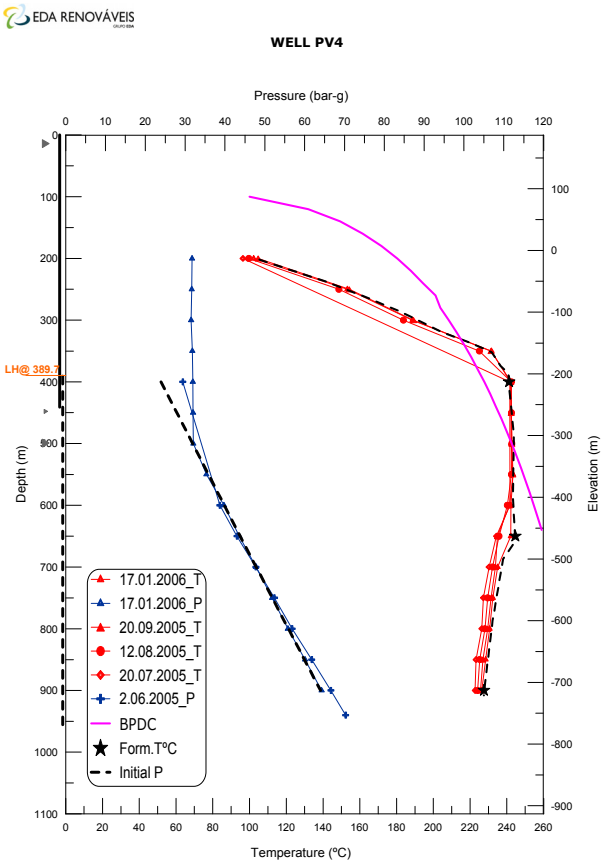

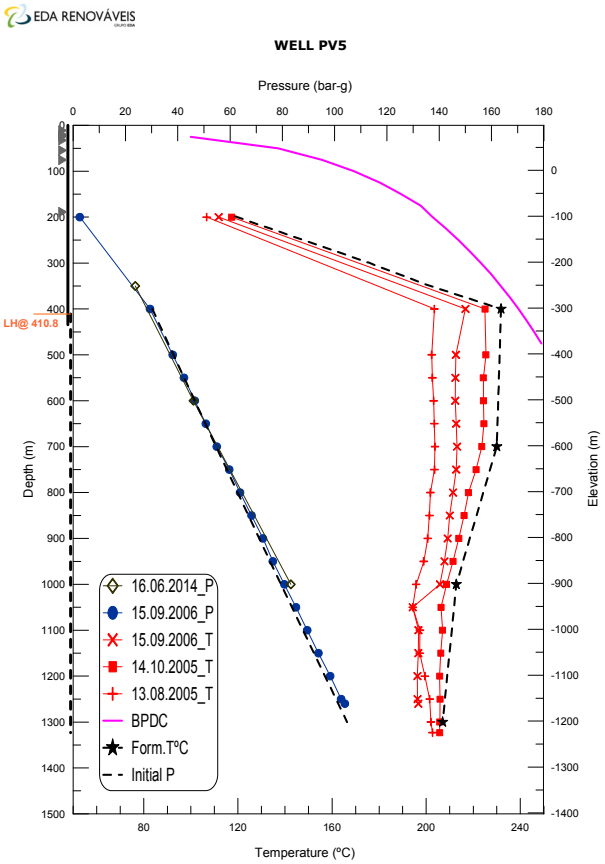

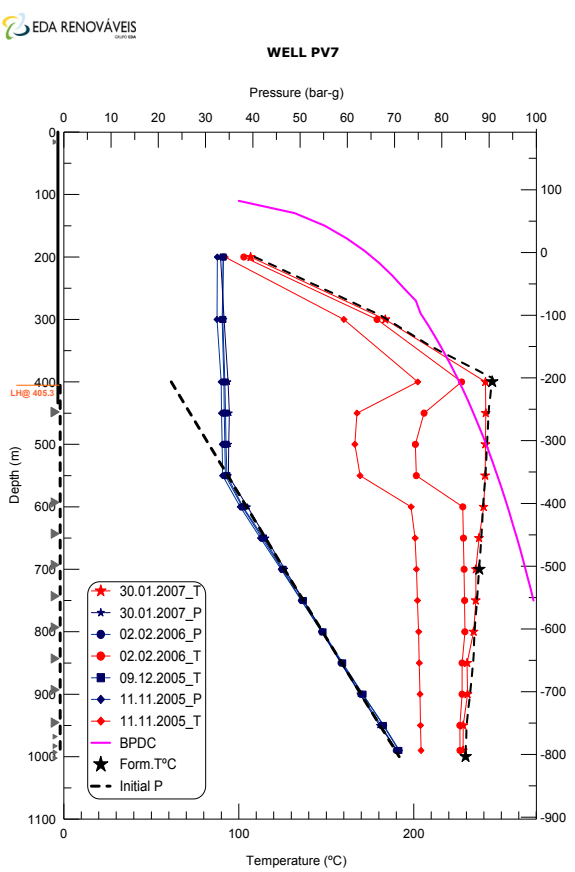
EDA RENOVÁVEIS
WELL PV7
Pressure (bar-g)
Depth (m)
Elevation (m)
Temperature (ºC)
LH@ 405.3
30.01.2007_T
30.01.2007_P
02.02.2006_P
02.02.2006_T
09.12.2005_T
11.11.2005_P
11.11.2005_T
BPDC
Form.TºC
Initial P

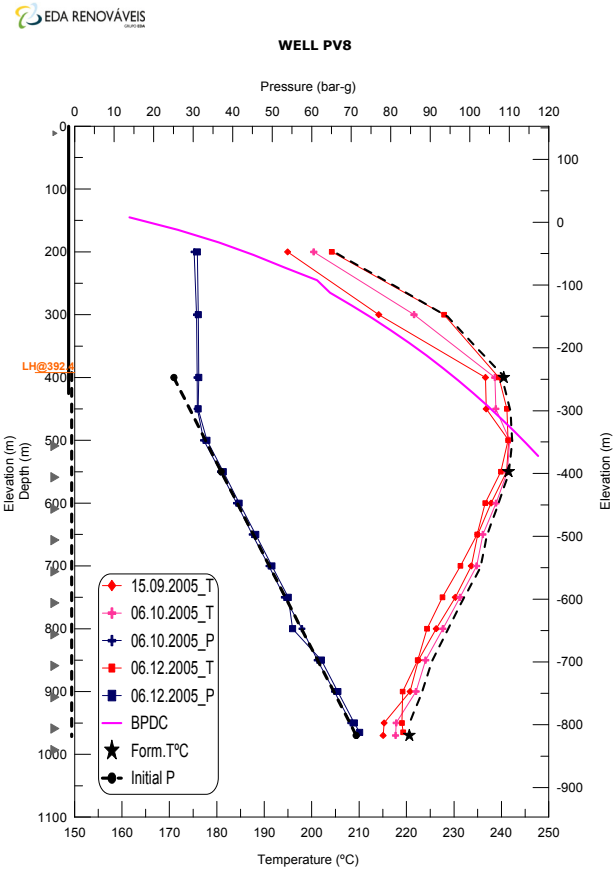
EDA RENOVÁVEIS
WELL PV8
Pressure (bar-g)
Depth (m)
Elevation (m)
Temperature (ºC)
LH@392.4
15.09.2005_T
06.10.2005_T
06.10.2005_P
06.12.2005_T
06.12.2005_P
BPDC
Form.TºC
Initial P